Journal of Ecology

Field evidence reveals conservative water use of poplars under high aerosol conditions in Beijing

Journal:	*Journal of Ecology*
Manuscript ID	JEcol-2020-1034.R1
Manuscript Type:	Research Article
Date Submitted by the Author:	10-Jan-2021

Complete List of Authors:	Wang, Bin; Institute of Botany Chinese Academy of Sciences, State Key Laboratory of Vegetation and Environmental Change; University of the Chinese Academy of Sciences Wang, Zhenhua; Institute of Botany Chinese Academy of Sciences, State Key Laboratory of Vegetation and Environmental Change; University of the Chinese Academy of Sciences Wang, Chengzhang; Institute of Botany Chinese Academy of Sciences, State Key Laboratory of Vegetation and Environmental Change; University of the Chinese Academy of Sciences Wang, Xin; Institute of Botany Chinese Academy of Sciences, State Key Laboratory of Vegetation and Environmental Change Li, Jing; Institute of Botany Chinese Academy of Sciences, State Key Laboratory of Vegetation and Environmental Change Beijing, CN Jia, Zhou; Institute of Botany Chinese Academy of Sciences, State Key Laboratory of Vegetation and Environmental Change; University of the Chinese Academy of Sciences Li, Ping; Institute of Botany Chinese Academy of Sciences, State Key Laboratory of Vegetation and Environmental Change; University of the Chinese Academy of Sciences Wu, Jin; University of Hong Kong, School of Biological Sciences Chen, Min; University of Wisconsin-Madison, Department of Forest and Wildlife Ecology Liu, Lingli; Institute of Botany Chinese Academy of Sciences, State Key Laboratory of Vegetation and Environmental Change

Key-words:	aerosols, ecophysiology, diffuse radiation, vapor pressure deficit, leaf temperature, sun and shade leaves, stomatal conductance, leaf transpiration, sap flow

Title: Field evidence reveals conservative water use of poplars under high aerosol conditions in Beijing

Authors:

Bin Wang[1, 2], Zhenhua Wang[1, 2], Chengzhang Wang[1, 2], Xin Wang[1], Jing Li[1, 2], Zhou Jia[1, 2], Ping Li[1, 2], Jin Wu[3], Min Chen[4], Lingli Liu[1, 2*]

Author affiliations:

[1] State Key Laboratory of Vegetation and Environmental Change, Institute of Botany, Chinese Academy of Sciences, Xiangshan, Beijing 100093, China

[2] University of Chinese Academy of Sciences, Yuquanlu, Beijing 100049, China

[3] School of Biological Sciences, The University of Hong Kong, Pokfulam, Hong Kong, China

[4] Department of Forest and Wildlife Ecology, University of Wisconsin-Madison, Madison, Wisconsin, USA

***Corresponding author:**

Lingli Liu

Tel: +86-10-62836160; Fax: +86-10-82596146; Email: lingli.liu@ibcas.ac.cn

Abstract

1. Anthropogenic aerosols could alter multiple meteorological processes such as radiation regime and air temperature, thereby modifying plant transpiration. However, the lack of field observations at leaf- and plant-level hinders our ability to understand how aerosols could affect plant water use.
2. Aerosol concentrations in northern China fluctuates periodically over a wide range. Taking advantage of this unique natural experiment opportunity, we conducted a full series of supporting physiological and environmental measurements to explore aerosols' effect on leaf transpiration and sap flow in the field using poplar trees (*Populus* × *canadensis* Moench).
3. We found that high aerosol concentrations suppressed sun-leaf transpiration by reducing leaf-to-air vapor pressure deficit (VPD_{leaf}), while had no effect on shade-leaf transpiration mainly because the negative effect of reduced VPD_{leaf} on transpiration offset the positive effects of the increased stomatal conductance (g_s). As aerosol concentration increases, the g_s of both sun and shade leaves decreased more rapidly with an increase in VPD_{leaf}, which caused their transpiration rates to become less sensitive to VPD_{leaf}. Similarly, aerosols reduced sap flow density and its sensitivity to VPD.
4. *Synthesis.* Our study provided observational evidence on aerosols' effects on plant transpiration at the leaf and canopy scales. The reduced transpiration and stronger stomatal control indicated that plant water use becomes more conservative under elevated aerosol concentrations.

Keywords:

aerosols, ecophysiology, diffuse radiation, vapor pressure deficit, leaf temperature, sun and shade leaves, stomatal conductance, leaf transpiration, sap flow

Introduction

Heavy aerosol pollution occurs widely in rapidly developing regions (such as East and South-East Asia), as well as regions under the influence of desert dust (such as the Sahara) or biomass burning (such as the Amazonia) (Yoon et al., 2014, Mehta et al., 2016). By scattering and absorbing solar radiation, aerosols reduce total radiation but enhance diffuse radiation, and thereby generally cool the atmosphere (Gu et al., 2003, Niyogi et al., 2004, Xia et al., 2007, Lu et al., 2017, Rap et al., 2018). Since both radiation regimes and air temperature have profound effects on stomatal behavior (Steiner and Chameides, 2005, Greenwald et al., 2006, Knohl and Baldocchi, 2008, Wang et al., 2018), aerosol induced changes in meteorological conditions could have complex impacts on leaf and canopy transpiration and thus plant water use. However, because few studies have been conducted with a full series of supporting physiological and environmental measurements, aerosol's effect on plant transpiration remains poorly understood.

The rate of plant transpiration is proportional to the leaf-to-air vapor pressure deficit (VPD_{leaf}) and the stomata conductance (g_s) (Pieruschka et al., 2010, McElrone et al., 2013, McDowell and Allen, 2015). Aerosols could decrease VPD_{leaf} due to its cooling effect and the accompanying high air humidity (Wang et al., 2018). The response of g_s to increased aerosol concentrations is likely more complicated due to potential variation in processes that mediate plant photosynthesis. Aerosols could stimulate the g_s of shade leaves as more diffuse light could illuminate the shade leaves and enhance their photosynthesis (Gu et al., 2003, Knohl and Baldocchi, 2008, Mercado et al., 2009). Aerosols may also stimulate the g_s of sun leaves because their photosynthesis rate could be enhanced by decreasing leaf temperatures (T_{leaf}) and alleviating the midday depression caused by supra-optimal T_{leaf} (Steiner and Chameides, 2005). The lower VPD_{leaf} under high aerosol loadings could reduce plant transpiration; alternatively, the higher g_s could stimulate it. These two processes simultaneously mediate plant water use, making it difficult to predict the response of plant transpiration to elevated aerosol concentrations.

Aerosol exposure may also alter the sensitivity of plant transpiration to atmospheric demand for water (usually characterized by VPD). The majority of anthropogenic aerosols are highly hygroscopic. The deliquescence of hygroscopic aerosols could establish a saturated water film connection between the leaf surface and the stomatal walls. The osmotic potential of the water film drives liquid water to the leaf surface and then evaporates into the atmosphere, which has been characterized as hydraulic activation of the stomata (HAS) (Burkhardt, 2010, Burkhardt et al., 2018). This HAS effect induced by aerosols could reduce stomatal control over plant water loss, and increase the minimum leaf conductance (Burkhardt, 2010, Burkhardt et al., 2018, Grantz et al., 2018), thereby reducing the tolerance of plants to meteorological drought (Burkhardt, 2010). However, as mentioned above, aerosol induces marked changes in radiation regime, VPD, and T_{leaf}, which could cause a faster and more substantial impact on plant transpiration (Steiner and Chameides, 2005, Knohl and Baldocchi, 2008, Kanniah et al., 2012, Wang et al., 2018), thereby counteracting or masking any effects of HAS. Even so, less attention has been paid to whether the increase in aerosol concentrations could affect the sensitivity of g_s and thus transpiration to meteorological drought. Climate changes will likely cause more frequent and severe meteorological drought in large areas of the world (Spinoni et al., 2020). Therefore, filling this knowledge gap is critical towards understanding plant water use efficiency in the future, considering the importance of meteorological drought in regulating stomatal behavior (Novick et al., 2016, Sulman et al., 2016, Yuan et al., 2019).

Furthermore, the direction and magnitude of aerosols' effect on plant transpiration rate could vary throughout the day. The diurnal patterns of transpiration rate depend upon a dynamic interaction between the endogenous physiological activities of the plant and the exogenous environmental conditions. Water transport within the plant root–xylem–leaf system has its endogenous diurnal rhythms (Du et al., 2011, Mallick et al., 2016). The effect of aerosols on radiation varies with the solar zenith angle (SZA). Compared to high SZA, aerosols cause a steeper decline in total radiation and a greater rise in diffuse radiation at low SZA conditions (Gu et al., 1999, Xia et al., 2007, Zhang et al., 2011). In other words, the effect of aerosols on the photosynthetically active radiation (PAR) received by leaves, and thus leaf g_s and transpiration, could be different as SZA varies from sunrise to sunset. Field observations are still needed to explore how aerosols could alter the dynamics of environmental factors and the responses of leaves and canopies over the day.

To investigate the effects of aerosols on plant water use under field conditions, we intensively measured meteorological conditions, leaf g_s, transpiration rate, and sap flow density of poplar trees (*Populus* × *canadensis* Moench) under natural *in-situ* aerosol exposure in Beijing, China, where the exceptionally wide range of aerosol fluctuations provided a unique opportunity to capture the response of plant transpiration to different aerosol concentrations (Guo et al., 2014, Wang et al., 2018). To avoid the confounding effects of seasonal variations in radiation, air temperature, plant phenology, and cloud cover, we only used the data measured during July and August under cloud-free skies. The strictly selected conditions ensured our study could effectively capture how aerosols affect leaf transpiration and sap flow density under natural conditions. We aimed to answer the following questions: How do elevated aerosol concentrations affect the meteorological conditions at different times of the day? How changes in meteorological conditions caused by elevated aerosol affect the diurnal course of transpiration of sun and shade leaves? Will aerosol exposure alter the sensitivity of leaf transpiration and sap flow density to changes in VPD?

Materials and Methods

Site description

The experimental site is located at the Forestry Experimental Station of the Institute of Botany, Chinese Academy of Sciences (39.98° N, 116.20° E, 74 m a.s.l.), Beijing, China. Climat at the site is temperate semi-humid monsoon, with a mean annual temperature of 13 °C and a mean annual precipitation of 600 mm. Figure S1 shows the annual variations of PAR, air temperature (T_{air}), precipitation, and relative humidity (RH) during the study period.

The high anthropogenic emissions and variation in atmospheric stability together cause the periodic fluctuations of aerosol concentrations in our study region (Guo et al., 2014, Fan et al., 2018). The aerosol optical depth (AOD), a measure of the extinction of solar radiation by aerosol particles (Ramanathan et al., 2001), ranged from 0.047 to 1.8 at our site during the study period.

Plant materials and experimental conditions

Poplar is the most widely planted deciduous tree species in China, with land area planted with poplars amounting to approximately 7.0 million hm^2 (Fang, 2008). Poplar is sensitive to atmospheric pollution and climate drought, making it an ideal study species to detect physiological responses to variations in aerosol concentrations (Karnosky et al., 2003, Wang et al., 2018, Wang et al., 2020). In this study, we chose a commonly planted hybrid poplar (*Populus*×*canadensis* Moench) as the model plant. We planted one *P*×*canadensis* Moench stand in 2011 with one-year-old seedlings and another stand in 2015 with two-year-old seedlings. The poplar seedlings of the two stands had the same provenience and were planted on the open ground with a spacing of 1m × 1m. The seedlings were watered during the first growing season after planting to ensure their survival.

During the study period, we measured tree height using an altimeter, the diameter of the stem at the breast height (DBH, 1 m above the ground) using an electronic vernier caliper, and the leaf area index (LAI) using an AccuPAR Ceptometer (LP80, Decagon Devices, Inc., Pullman WA, USA). We also used an increment borer to take the increment cores and used an electronic vernier caliper to measure the depth of the sapwood. The average height, DBH, LAI, and sapwood thickness of the studied trees during each measurement year were shown in Table S1.

Measurements of aerosol concentration and meteorological conditions

Particulate matter less than 2.5 μm in aerodynamic diameter (PM2.5, μg m^{-3}) is the main component of the anthropogenic aerosols in our study area, and is highly correlated with AOD ($R^2 = 0.73$, Figure S2). In this study, we used the level of AOD at 500 nm and PM2.5 concentration as the indicators for aerosol loading. The AOD at 500 nm was manually measured each hour from 08:00 to 17:00 by a hand-held sun photometer (MICROTOPS II, Solar Light Company, Glenside, PA, USA) during cloud-free days in 2014 and 2015. The PM2.5 concentration was automatically measured every hour by Tapered Element Oscillating Microbalances (TEOM, RP1400a, Thermo Electron Corp., Beverly, MA, USA) at the air quality monitoring station of the Beijing Municipal Environmental Monitoring Center (BJMEMC, www.bjmemc.com.cn), located 1 km away from our study site.

A weather monitoring system (EM50, Decagon Devices Inc., Pullman WA, USA) was mounted on the open ground at a height of 2 m to continuously monitor meteorological variables, including precipitation (measured using a High Resolution Rain Gauge, ECRN-100, Decagon Devices Inc., Pullman WA, USA), PAR (measured using a sensor with leveling plate, SP-110, Apogee Instruments Inc., Logan UT, USA), air temperature and relative humidity (measured using a Temperature & Relative Humidity sensor, VP-3, Decagon Devices Inc., Pullman WA, USA), and soil moisture at depths of 15 cm and 40 cm (measured using a Water Content and Temperature sensor, 5TM, Decagon Devices Inc., Pullman WA, USA). All these variables were measured every 30 seconds, and were recorded as 30-minute averages by a data logger. We also monitored the total, diffuse and direct radiation (W m^{-2}) received by the land surface of the site using a Sunshine Pyranometer (SPN1, Delta-T Devices Ltd, Burwell Cambridge, UK), which were sampled every 10 seconds and recorded as 30-minute averages. VPD was calculated using the measured air temperature and relative humidity.

Measurements of leaf transpiration rate, g_s, and microclimate

Leaf transpiration rates were measured hourly from 08:00 to 17:00 during cloud-free days using a Portable Photosynthesis System (LI-6400, LICOR Inc., Lincoln NE, USA) in 2014 and 2015 at the poplar stand planted in 2011. Three healthy sun and shade leaves with similar size and phenology stages located in different branches were randomly selected. The sun leaves were recently matured, located in the third to the fifth position from the apex of the branch. The shade leaves were fully matured and completely shaded inside the canopy. During each measurement date, the selected leaves were measured every hour in a fixed order. Measurements usually stabilized in 3 minutes after clamping the leaf in the chamber, and the data were logged when fluxes were stable over 10 seconds.

PAR received by the leaves, VPD_{leaf}, T_{leaf}, and air vapor content (AVC) were simultaneously measured by self-contained sensors of LI-6400 when measuring leaf transpiration rates. Sun leaf transpiration rates were measured in 2014 and 2015, but shade leaf transpiration rates were only measured in 2015. To minimize the effects of leaf phenology, we only used the data collected during July and August. The dynamics of daily AOD, PAR, air temperature, and RH during cloud-free days from July to August in 2014 and 2015 were shown in Figure S3.

Measurements of stem sap flow density

We selected 5 healthy trees with similar DBH and height from the stand planted in 2015, and measured their sap flow density using the thermal dissipation probe method (TDP) in 2017 and 2018. For each selected tree, a pair of TDP probes with a diameter of 2 mm (TDP30, Dynamax Inc., Houston TX, USA) were inserted into the sapwood of the north side of the stem. The sapwood thickness of the studied trees ranged from 34.4 to 37.6 mm (Table S1). The TDP probes we used were 30 mm long, which ensured the sap flow density of the sapwood could be effectively captured. The upper probe was heated with a constant power of 0.20 W, and the lower probe served as a temperature reference. The temperature difference between the two probes is influenced by the heat dissipation of the sapwood due to water flux. When the water flux in the sapwood is high, the heat dissipation cools the heat source in the upper probe, reducing the temperature difference between the two probes. When the sap flow density is zero or minimal in the nighttime, the temperature difference between the two probes is maximal (Granier, 1987). Because we used needles with smaller diameters than previous studies, we installed the paired probes with a shorter distance (4 cm) than these studies (10-15 cm) (Granier, 1987, Clausnitzer et al., 2011). The shorter distance reduced the natural thermal gradient, but could result in the heating of the up probe diffuses to the down one, especially during nighttime. Because aerosols' impact on sap flow mainly occurred during noontime, this short distance should have a small impact on our findings.

Both probes contained a copper-constantan thermocouple (T-type thermocouple) in the middle to detect the temperature around the probes. An aluminum box covered the sensor to prevent the disturbances of radiation, rainfall, and physical damages. The temperature difference between the two probes was measured every 30 seconds, and 30-minute averages were recorded by a data logger (DT80, Thermo Fisher Scientific, Waltham, MA, USA). Sap flow density was calculated with the Granier empirical equation:

$$SFD = 119 \times 10^{-6} \times \left(\frac{\Delta T_M - \Delta T}{\Delta T}\right),$$

where SFD (g m^{-2} s^{-1}) is the sap flow density, ΔT_M (K) is the maximal temperature difference, and ΔT (K) is the measured temperature difference. The relationship between SFD and temperature difference is conversed by an empirical coefficient of 119×10^{-6} (Granier, 1987). Granier (1987) assumed that ΔT_M occurs every night when the sap flux reached zero. However, many studies have proved that the sap flow can continue throughout the night (Fisher et al., 2007, Zeppel et al., 2010). To improve the estimation of ΔT_M, we adopted the commonly used empirical moving window approach, which assumes that zero flux occurs only once within the selected time window (Moore et al., 2008, Clausnitzer et al., 2011, Rabbel et al., 2016). In our study, we used a five-day moving window to determine ΔT_M so that the nocturnal sap flow could be effectively captured and the influence of data drift would be reduced.

Statistical analysis

Diurnal dynamics of meteorological factors and leaf transpiration under different AOD conditions

According to the Environmental Protection Control Standard of China, air quality can be broken down into different categories by the air quality index (AQI) scores (Hu et al., 2015). Based on these scores, the daily mean AOD at our study site during cloud-free days fell within three categories: excellent (0.1-0.3), good (0.3-0.6), and lightly polluted (0.6-1.6). It should be noted that the true "zero level" of AOD is hard to monitor in the field because anthropogenic and natural sources continue to emit gaseous precursors and aerosol particles into the atmosphere. To illustrate the diurnal course of meteorological variables and leaf transpiration under different aerosol conditions, we grouped the observations for each hour by three intervals (0.1-0.3, 0.3-0.6, and 0.6-1.6) according to their AQI categories. The interval of AOD in 0.3-0.6 was absent for shade leaves because there was only one cloud-free day with AOD falling within the range of 0.3 to 0.6 in 2015.

Before proceeding with further statistical analysis, data were tested for normality of distribution and homogeneity of variance using the Shapiro-Wilk test and Bartlett test, respectively. The non-normally distributed data were log-transformed to ensure normality. One-way analysis of variance (ANOVA) was used to test whether aerosol concentrations had a significant impact on radiation, air temperature, PAR received by leaves, VPD_{leaf}, T_{leaf}, AVC, and leaf transpiration for each hour from 8:00 to 17:00 of the day.

The response of g_s and leaf transpiration to changes in aerosol concentrations

We further explored the underlying mechanisms that drove the changes in transpiration of sun and shade leaves. We only used observations around noontime (11:00–14:00 with SZA less than 40 degrees) for these analyses to reduce the confounding influence of the diurnal rhythm of leaf water potential. Linear regression was used to reveal the effect of aerosol loading on leaf transpiration rate, $VPD_{leaf,}$ and g_s, respectively. Structural equation modeling (SEM) is a useful statistical procedure for assessing inter-relationships among observed variables (Grace, 2006). We conducted SEM to examine the causal pathways via which aerosol concentrations affected meteorological factors (PAR, $T_{air,}$ and VPD_{leaf}) and thus T_{leaf} and g_s.

The sensitivity of leaf water use to VPD under different aerosol conditions

To test whether aerosol loading can alter the sensitivity of leaf water use to VPD, we regressed transpiration and g_s against VPD_{leaf} for each AOD interval around noontime. We then conducted ANCOVA using the 'HH' package in R (Heiberger, 2016) to compare the slopes of the regressions between different AOD intervals. To further test whether changes in the meteorological condition under different aerosol loading could contribute to the changes in sensitivity of water use to VPD, we partitioned the range of the PAR and T_{leaf} level into 4 to 6 intervals of equal width. We then regressed g_s against VPD_{leaf} for each PAR/T_{leaf} interval and test the statistical difference of regression slopes between different intervals by ANCOVA.

The response of sap flow density to changes in aerosol concentrations

To explore the effect of aerosol loadings on sap flow density, we selected the sap flow data collected during cloud-free and windless days from June and August in 2017 and 2018. Because it was difficult to match the high-frequency sap flow data with manually measured AOD, we matched the sap flow data with the automatic monitored PM2.5 concentration since it was highly correlated with AOD at our site (Figure S2). We calculated the averages of sap flow density, PM2.5 concentration, and VPD for 24 hours (00:00–24:00). The first-order difference was used to remove the influence of seasonal trends in PM2.5 concentrations, sap flow density, VPD, and radiation (Wang et al., 2018). To investigate the difference of sap flow among different aerosol conditions, we further partitioned the range of daily PM2.5 concentrations (μg m^{-3}) into 4 intervals (0-20, 20-40, 40-60 and 60-80 μg m^{-3}) and regressed sap flow density against VPD for each PM2.5 interval. We then assessed whether aerosol exposure altered the sensitivity of canopy water use to VPD by comparing the slopes at different PM2.5 intervals using ANCOVA.

All analysis was conducted in the software R 3.6.1 (R Core Development Team, 2019).

Results

Meteorological conditions under different aerosol loadings

When analyzing the meteorological data on an hourly basis during the daytime (from 08:00 to 17:00), the total radiation and direct radiation decreased significantly with increasing AOD in most hours. In contrast, the diffuse radiation increased substantially with increasing AOD at all hours (Figure 1a-c). Except for 08:00 and 12:00, air temperature at all other hours decreased significantly with the increase of AOD (Figure 1d).

As AOD increased, PAR received by sun leaves decreased throughout the day (Figure 2a), but PAR received by shade leaves increased except for the late afternoon (Figure 2b). Leaf temperature (T_{leaf}) for sun leaves decreased with AOD except for morning hours (Figure 2c), but T_{leaf} for shade leaves was less affected by AOD (Figure 2d). High AOD was accompanied by high AVC (Figure S4). Together, these changes in T_{leaf} and AVC decreased VPD_{leaf} under elevated aerosol concentrations for both sun and shade leaves (Figures 2e-f, S5).

Aerosol effects on leaf transpiration rate and g_s

Aerosol exposure reduced sun leaves' transpiration rate throughout the day, with the most considerable suppression around midday (Figures 3a, S6a). High AOD tended to increase the transpiration rate of shade leaves, but the effect was significant only at noon (Figures 3b, S6b).

The transpiration rate of sun leaves around midday decreased by 0.23 mmol H_2O m^{-2} s^{-1} for every 0.1 increase in AOD (Figure 4a). The reduced sun-leaf transpiration rate corresponded to a decrease in $VPD_{leaf,}$ while g_s did not change (Figure 4c,e). With the increase in AOD, the VPD_{leaf} of shade leaves decreased, but g_s increased (Figure 4d,f). No significant correlation between the transpiration rate of shade leaves and AOD was observed (Figure 4b). During our measurements, soil moisture did not vary with AOD and had no significant influence on transpiration (Figure S7).

The effects of aerosols on the sensitivity of leaf transpiration and g_s to VPD_{leaf}

The ANCOVA demonstrated that microclimate (PAR, $T_{leaf,}$ and VPD_{leaf}) showed similar responses to changes in aerosol concentrations under different AOD conditions (Figure S8). However, aerosol exposure altered the sensitivity of sun-leaf transpiration to VPD_{leaf}, with a positive response to VPD_{leaf} under low aerosol conditions, but no response under medium and high aerosol conditions (Figure 5a). The response of shade-leaf transpiration to VPD_{leaf} was not significantly different between the low and high aerosol conditions (Figure 5b). As aerosol concentration increases, the g_s of both sun and shade leaves became more responsive to VPD_{leaf}. Compared to low aerosol conditions, sun leaf g_s declined more rapidly with increasing VPD_{leaf} under medium and high aerosol conditions (Figure 5c). Similar trends were observed for shade leaves, although the ANCOVA indicated that their responses were not statistically different under different aerosol conditions (Figure 5d).

Sun leaves received less PAR and had lower T_{leaf} under higher aerosol conditions (Figure 2a,c). The g_s of sun leaves showed a negative response to VPD_{leaf} when PAR was less than 1800 μmol m^{-2} s^{-1}, but had no response to VPD_{leaf} when PAR exceeded 1800 μmol m^{-2} s^{-1} (Figure 6a). The sensitivity of sun-leaf g_s to VPD_{leaf} decreased with an increase in T_{leaf} ($P < 0.001$). When T_{leaf} exceeded 37 °C, sun-leaf g_s no longer responded to changes in VPD_{leaf} (Figure 6c). Shade leaves received more PAR under high aerosol conditions (Figure 2b). The ANCOVA demonstrated that the sensitivity of shade-leaf g_s to VPD_{leaf} was enhanced significantly with the increase in PAR (*P* < 0.001, Figure 6b), but was not affected by changes in T_{leaf} (*P* = 0.88, Figure 6d).

Aerosol effects on sap flow density

There was a significant negative correlation between detrended daily sap flow density and detrended daily PM2.5 concentrations (Figure 7a). In contrast, detrended sap flow density increased with detrended VPD. However, the sensitivity of sap flow density to VPD declined under higher PM2.5 conditions, as the ANCOVA demonstrated that the slopes between sap flow density and VPD decreased at higher PM2.5 (Figure 7b).

Discussion

In this study, we monitored leaf transpiration, sap flow density, and meteorological conditions in the field under a wide range of aerosol concentrations during cloud-free days. Consistent with previous studies (Mercado et al., 2009, Doughty et al., 2010, Kanniah et al., 2012), we found that aerosols significantly reduced air temperature and PAR received by sun leaves, but increased PAR received by shade leaves because of the diffuse radiation fertilization effect (Figures 1, 2). The changes in canopy light condition and air temperature could greatly alter the microclimate of sun and shade leaves (Steiner and Chameides, 2005, Knohl and Baldocchi, 2008, Wang et al., 2018). Indeed, our SEM analyses indicated that aerosol's cooling effect on air temperature indirectly reduced T_{leaf} for both sun and shade leaves (Figures S9, S11). An increase in aerosol concentration also altered the transpiration rates of sun and shade leaves and thus indirectly affected their T_{leaf}. However, the standardized total effect of T_{air} on T_{leaf} was much greater than that of leaf transpiration (Figure S9), suggesting that T_{leaf} was mainly affected by the exchange of sensible heat flux between leaf and air, rather than the cooling effect of transpiration.

Both VPD_{leaf} and PAR could greatly influence leaf g_s (Jarvis, 1976, Gao et al., 2002, Medlyn et al., 2011). The decrease in T_{leaf} and the accompanying high air humidity resulted in a significant reduction in VPD_{leaf} for both sun and shade leaves under high aerosol conditions (Figures 2, S5). For the sun leaves, aerosol exposure did not alter their g_s because the positive effect caused by lower VPD_{leaf} offset the negative effect caused by the decrease in PAR received by sun leaves (Figure S10a). For the shade leaves, due to the dual positive effects of reducing VPD_{leaf} and increased leaf received PAR, aerosol exposure increased the g_s of shade leaves (Figure S10b). Since g_s of sun leaf was not changed, the decrease in VPD_{leaf} under high aerosol conditions significantly reduced sun-leaf transpiration (Figure 4a,c,e); Whereas the lack of response in shade leaf transpiration was due to the negative effect of lower VPD_{leaf} offsetting the positive effect of enhanced shade leaf g_s (Figure 4b,d,f). In addition to VPD, soil moisture is another critical factor regulating g_s (Emanuel et al., 2007, Novick et al., 2016). However, as the study was conducted during the rainy season, soil moisture was maintained at a relatively stable level (0.15-0.20 m^3 m^{-3}) and had no significant influence on transpiration (Figure S7).

Furthermore, we also found that aerosols' effect on transpiration was largest around midday (Figures 3, S6). This was mainly because the effect of aerosols on radiation was larger when the solar zenith angle was low (Gu et al., 1999, Xia et al., 2007, Zhang et al., 2011), and thus induced more significant changes in leaf micro-climate conditions, such as PAR, T_{leaf}, and VPD_{leaf} (Figures 2, S3). Because sun leaf transpiration decreased throughout the day, while shade leaf transpiration only increased around midday, we expected that aerosol loading would reduce canopy transpiration, rather than increase it as predicted by most model studies (Steiner and Chameides, 2005, Knohl and Baldocchi, 2008, Liu et al., 2014, Lu et al., 2017). Indeed, our observations of stem sap flow confirmed this expectation: as aerosol loading increased, the daily average sap flow density decreased (Figures 7a, S12). However, the decrease in sap flow density could be because our young poplar trees have a relatively simple canopy structure, and sun leaf response played a dominant role in driving the whole tree transpiration (Knohl and Baldocchi, 2008, Lu et al., 2017). Unlike the young poplar plantation in our study, the natural forests are composed of trees with diverse ages and species and thus have a more complex canopy structure. As our field observation revealed that sun and shade leaf transpiration showed different response to increase in aerosol concentrations, we believed that improving the model representation of the sun and shade leaf fraction along the canopy vertical profile (Wu et al., 2017) should significantly improve the simulation of natural forest transpiration under elevated aerosols.

In addition, our field observations further found that aerosol loading enhanced stomatal sensitivity to VPD_{leaf} for both sun and shade leaves around midday (Figure 5c,d). The more effective stomatal control could be because aerosol loading altered micro-meteorological conditions within the canopy. For sun leaves, high aerosol loading resulted in a rapid decline in PAR received by the leaf surface, thereby reducing T_{leaf} (Figure 6a,c). Previous works suggested that stomata have a slow response to environmental stimuli when leaf temperature is between 35 and 50°C (Wang et al., 2007, Weston and Bauerle, 2007, Ameye et al., 2012). In our study, we found that when temperature was higher than 35.5 ℃, sun leaf photosynthesis began to decline (Figure S13). The reduced stomatal control under high T_{leaf} (>35.5 ℃) could be due to the combined effects of the reduced carboxylation capacity and the accompanied low VPD (Lloyd, 1991, Medlyn et al., 2011, Novick et al., 2016). High aerosol loading mitigated the heat stress for sun leaves and thus increased the sensitivity of g_s to changes in VPD_{leaf}. For shade leaves, where g_s is usually strongly limited by the low light inside the canopy, the increased sensitivity of g_s to VPD_{leaf} appeared mainly because the aerosol-induced diffuse fertilization effect stimulated stomatal opening (Knohl and Baldocchi, 2008, Mercado et al., 2009, Wang et al., 2018). The enhanced blue light under aerosol loadings may also contribute to the stomatal response by regulating aperture (Urban et al., 2007, Dengel and Grace, 2010), although we did not test that here. The increased stomatal control under high aerosol loading weakened the response of leaf transpiration to VPD_{leaf}, although the impact was significant only for sun leaves (Figure 5a,b).

Similarly, at the canopy level, sap flow density was less sensitive to increased VPD under high aerosol loadings (Figure 7b).

Previous research suggested that by establishing a saturated water film on the leaf surface, the aerosol-induced HAS effect could cause an increase in plant water loss (Burkhardt et al., 2001, Burkhardt, 2010, Grantz et al., 2018). Instead, we found that aerosol loading actually reduced sun leaf transpiration and sap flow (Figures 4a, 7a). Also, the HAS effect is expected to cause a weakened response of stomata to changes in VPD by decoupling leaf transpiration from stomatal aperture (Burkhardt et al., 2001, Grantz et al., 2018). However, our observation showed that under high aerosol loadings, g_s was more sensitive to changes in VPD_{leaf} (Figure 5c,d), implying stronger stomatal control of transpiration under meteorological drought. Our findings indicate that plants have more conservative water use under high aerosol concentrations, which contradicts the predictions of the HAS effect (Grantz et al., 2018). This difference could be because aerosol-induced radiation regime changes greatly alter meteorological conditions, such as reducing T_{leaf} and VPD_{leaf} during the day time. These changes in meteorological conditions predominantly drive the response of g_s and transpiration, thereby masking the impacts caused by HAS. The strength of HAS on plant water loss also depends on plant water-use strategies, such as isohydric and anisohydric stomata regulation (Burkhardt and Pariyar, 2016), as well as leaf traits such as trichomes, epicuticular wax, and the morphology and orientation of the leaves (Burkhardt, 2010).

All these factors could alter the impact magnitude of HAS on plant transpiration but were beyond the scope of this work.

Conclusions

In summary, our study provided observational evidence on the effects of aerosols on plant water use at the leaf and canopy scales. Although aerosol-induced changes in meteorological conditions increased leaf and canopy photosynthesis at our site (Wang et al., 2018), the increased photosynthesis was accompanied by more conservative water use by plants, suggesting that elevated aerosol concentration might increase plant water use efficiency. Our empirical observations of the diurnal dynamics of the transpiration of sun leaves, shade leaves, and the canopy should be useful for improving models of plant transpiration under elevated aerosols. Meanwhile, the responses of plant transpiration to aerosol concentrations are determined by a combination of various environmental stimuli and hydrological functional properties of plants. Changes in radiation regime, canopy microclimate, and HAS could induce different impacts in different species or ecosystems. Furthermore, high aerosol pollution is usually accompanied by high nitrogen deposition (Huang et al., 2014), and nitrogen deposition can alter g_s and thus transpiration by changing leaf nutrient status (Liang et al., 2020). More experimental studies in natural forests are needed, integrating leaf-, canopy-, and ecosystem-scale observations to better reveal how aerosols and their interactions with climate changes and other air pollutants could affect plant water use.

Acknowledgment

This study was financially supported by the National Natural Science Foundation of China (31670478, 31600389, 31988102, 31522011).

Conflicts of interest

The authors declare that there is no conflict of interest.

Author contributions

L.L.L., B.W., and Z.H.W. designed the experiment. B.W., Z.H.W., C.Z.W., J.L., and Z.J. performed the experiment. B.W. and L.L.L analyzed the data and wrote the manuscript. Z.H.W, X.W., P.L., J.W., and M.C. commented on the details of the manuscript drafts.

Data availability statement

Data are available from the Dryad Digital Repository https://doi.org/10.5061/dryad.wh70rxwmn (Wang et al., 2021).

References

Ameye, M., Wertin, T. M., Bauweraerts, I., McGuire, M. A., Teskey, R. O. & Steppe, K. (2012) The effect of induced heat waves on Pinus taeda and Quercus rubra seedlings in ambient and elevated CO2 atmospheres. *New Phytologist,* **196,** 448-461.

Buckley, T. N., Sack, L. & Farquhar, G. D. (2017) Optimal plant water economy. *Plant Cell Environ,* **40,** 881-896.

Burkhardt, J. (2010) Hygroscopic particles on leaves: nutrients or desiccants? *Ecological Monographs,* **80,** 369-399.

Burkhardt, J., Kaiser, H., Kappen, L. & Goldbach, H. E. (2001) The possible role of aerosols on stomatal conductivity for water vapour. *Basic and Applied Ecology,* **2,** 351-364.

Burkhardt, J. & Pariyar, S. (2016) How does the VPD response of isohydric and anisohydric plants depend on leaf surface particles? *Plant Biol (Stuttg),* **18 Suppl 1,** 91-100.

Burkhardt, J., Zinsmeister, D., Grantz, D. A., Vidic, S., Sutton, M. A., Hunsche, M. & Pariyar, S. (2018) Camouflaged as degraded wax: hygroscopic aerosols contribute to leaf desiccation, tree mortality, and forest decline. *Environmental Research Letters,* **13,** 085001.

Clausnitzer, F., Köstner, B., Schwärzel, K. & Bernhofer, C. (2011) Relationships between canopy transpiration, atmospheric conditions and soil water availability—Analyses of long-term sap-flow measurements in an old Norway spruce forest at the Ore Mountains/Germany. *Agricultural and Forest Meteorology,* **151,** 1023-1034.

Dengel, S. & Grace, J. (2010) Carbon dioxide exchange and canopy conductance of two coniferous forests under various sky conditions. *Oecologia,* **164,** 797-808.

Doughty, C. E., Flanner, M. G. & Goulden, M. L. (2010) Effect of smoke on subcanopy shaded light, canopy temperature, and carbon dioxide uptake in an Amazon rainforest. *Global Biogeochemical Cycles,* **24,** GB3015.

Du, S., Wang, Y.-L., Kume, T., Zhang, J.-G., Otsuki, K., Yamanaka, N. & Liu, G.-B. (2011)

Sapflow characteristics and climatic responses in three forest species in the semiarid Loess Plateau region of China. *Agricultural and Forest Meteorology,* **151,** 1-10.

Emanuel, R. E., D'Odorico, P. & Epstein, H. E. (2007) A dynamic soil water threshold for vegetation water stress derived from stomatal conductance models. *Water Resources Research,* **43**.

Fan, T., Liu, X., Ma, P., Zhang, Q., Li, Z., Jiang, Y., Zhang, F., Zhao, C., Yang, X., Wu, F. & Wang, Y. (2018) Emission or atmospheric processes? An attempt to attribute the source of large bias of aerosols in eastern China simulated by global climate models. *Atmospheric Chemistry and Physics,* **18,** 1395-1417.

Fang, S. Z. (2008) Silviculture of poplar plantation in China: a review. *Ying yong sheng tai xue bao = The journal of applied ecology,* **19,** 2308-16.

Fisher, J. B., Baldocchi, D. D., Misson, L., Dawson, T. E. & Goldstein, A. H. (2007) What the towers don't see at night: nocturnal sap flow in trees and shrubs at two AmeriFlux sites in California. *Tree Physiology,* **27,** 597-610.

Gao, Q., Zhao, P., Zeng, X., Cai, X. & Shen, W. (2002) A model of stomatal conductance to quantify the relationship between leaf transpiration, microclimate and soil water stress. *Plant, Cell and Environment*.

Grace, J. B. (2006) Structural Equation Modeling and Natural Systems. *Cambridge University Press*.

Granier, A. (1987) Evaluation of transpiration in a Douglas-fir stand by means of sap flow measurements. *Tree Physiology,* **3,** 309-319.

Grantz, D. A., Zinsmeister, D. & Burkhardt, J. (2018) Ambient aerosol increases minimum leaf conductance and alters the aperture-flux relationship as stomata respond to vapor pressure deficit (VPD). *New Phytologist,* **219,** 275-286.

Greenwald, R., Bergin, M. H., Xu, J., Cohan, D., Hoogenboom, G. & Chameides, W. L. (2006) The influence of aerosols on crop production: A study using the CERES crop model. *Agricultural Systems,* **89,** 390-413.

Gu, L., Baldocchi, D. D., Wofsy, S. C., Munger, J. W., Michalsky, J. J., Urbanski, S. P. & Boden, T. A. (2003) Response of a deciduous forest to the Mount Pinatubo eruption: enhanced photosynthesis. *Science,* **299,** 2035-8.

Gu, L., Fuentes, J. D., Shugart, H. H., Staebler, R. M. & Black, T. A. (1999) Responses of net ecosystem exchanges of carbon dioxide to changes in cloudiness: Results from two North American deciduous forests. *Journal of Geophysical Research,* **104,** 31421-31434.

Guo, S., Hu, M., Zamora, M. L., Peng, J., Shang, D., Zheng, J., Du, Z., Wu, Z., Shao, M., Zeng, L., Molina, M. J. & Zhang, R. (2014) Elucidating severe urban haze formation in China. *Proceedings of the National Academy of Sciences of the United States of America,* **111,** 17373-17378.

Heiberger, R. M. (2016) HH: Statistical Analysis and Data Display: Heiberger and Holland. *R* *package version 3.1-32*.

Hu, J., Ying, Q., Wang, Y. & Zhang, H. (2015) Characterizing multi-pollutant air pollution in China: Comparison of three air quality indices. *Environment International,* **84,** 17-25.

Huang, R.-J., Zhang, Y., Bozzetti, C., Ho, K.-F., Cao, J.-J., Han, Y., Daellenbach, K. R., Slowik, J. G., Platt, S. M., Canonaco, F., Zotter, P., Wolf, R., Pieber, S. M., Bruns, E. A., Crippa, M., Ciarelli, G., Piazzalunga, A., Schwikowski, M., Abbaszade, G., Schnelle-Kreis, J., Zimmermann, R., An, Z., Szidat, S., Baltensperger, U., El Haddad, I. & Prevot, A. S. H. (2014) High secondary aerosol contribution to particulate pollution during haze events in China. *Nature,* **514,** 218-222.

Jarvis, P. G. (1976) The Interpretation of the Variations in Leaf Water Potential and Stomatal Conductance Found in Canopies in the Field.

Kanniah, K. D., Beringer, J., North, P. & Hutley, L. (2012) Control of atmospheric particles on diffuse radiation and terrestrial plant productivity: A review. *Progress in Physical Geography,* **36,** 209-237.

Karnosky, D. F., Zak, D. R., Pregitzer, K. S., Awmack, C. S., Bockheim, J. G., Dickson, R. E., Hendrey, G. R., Host, G. E., King, J. S., Kopper, B. J., Kruger, E. L., Kubiske, M. E., Lindroth, R. L., Mattson, W. J., McDonald, E. P., Noormets, A., Oksanen, E., Parsons, W. F. J., Percy, K. E., Podila, G. K., Riemenschneider, D. E., Sharma, P., Thakur, R., Sober, A., Sober, J., Jones, W. S., Anttonen, S., Vapaavuori, E., Mankovska, B., Heilman, W. &

Isebrands, J. G. (2003) Tropospheric O-3 moderates responses of temperate hardwood forests to elevated CO2: a synthesis of molecular to ecosystem results from the Aspen FACE project. *Functional Ecology,* **17,** 289-304.

Knohl, A. & Baldocchi, D. D. (2008) Effects of diffuse radiation on canopy gas exchange processes in a forest ecosystem. *Journal of Geophysical Research,* **113,** G02023.

Liang, X., Zhang, T., Lu, X., Ellsworth, D. S., BassiriRad, H., You, C., Wang, D., He, P., Deng, Q., Liu, H., Mo, J. & Ye, Q. (2020) Global response patterns of plant photosynthesis to nitrogen addition: A meta-analysis. *Glob Chang Biol,* **26,** 3585-3600.

Liu, S., Chen, M. & Zhuang, Q. (2014) Aerosol effects on global land surface energy fluxes during 2003-2010. *Geophysical Research Letters,* **41,** 7875-7881.

Lloyd, J. (1991) Modelling stomatal responses to environment in Macadamia integrifolia. *Australian Journal of Plant Physiology,* **18,** 649-660.

Lu, X., Chen, M., Liu, Y., Miralles, D. G. & Wang, F. (2017) Enhanced water use efficiency in global terrestrial ecosystems under increasing aerosol loadings. *Agricultural and Forest Meteorology,* **237-238,** 39-49.

Mallick, K., Trebs, I., Boegh, E., Giustarini, L., Schlerf, M., Drewry, D. T., Hoffmann, L., von Randow, C., Kruijt, B., Araujo, A., Saleska, S., Ehleringer, J. R., Domingues, T. F., Ometto, J. P. H. B., Nobre, A. D., Leal de Moraes, O. L., Hayek, M., Munger, J. W. & Wofsy, S. C. (2016) Canopy-scale biophysical controls of transpiration and evaporation in the

Amazon Basin. *Hydrology and Earth System Sciences,* **20,** 4237-4264.

McDowell, N. G. & Allen, C. D. (2015) Darcy's law predicts widespread forest mortality under climate warming. *Nature Climate Change,* **5,** 669-672.

McElrone, A. J., Choat, B., Gambetta, G. A. & Brodersen, C. R. (2013) Water uptake and transport in vascular plants. *Nature Education Knowledge,* **4,** 6.

Medlyn, B. E., Duursma, R. A., Eamus, D., Ellsworth, D. S., Prentice, I. C., Barton, C. V. M., Crous, K. Y., De Angelis, P., Freeman, M. & Wingate, L. (2011) Reconciling the optimal and empirical approaches to modelling stomatal conductance. *Global Change Biology,* **17,** 2134-2144.

Mehta, M., Singh, R., Singh, A., Singh, N. & Anshumali (2016) Recent global aerosol optical depth variations and trends — A comparative study using MODIS and MISR level 3 datasets. *Remote Sensing of Environment,* **181,** 137-150.

Mercado, L. M., Bellouin, N., Sitch, S., Boucher, O., Huntingford, C., Wild, M. & Cox, P. M. (2009) Impact of changes in diffuse radiation on the global land carbon sink. *Nature,* **458,** 1014-7.

Moore, G. W., Cleverly, J. R. & Owens, M. K. (2008) Nocturnal transpiration in riparian Tamarix thickets authenticated by sap flux, eddy covariance and leaf gas exchange measurements. *Tree Physiology,* **28,** 521-528.

Niyogi, D., Chang, H. I., Saxena, V. K., Holt, T., Alapaty, K., Booker, F., Chen, F., Davis, K. J., Holben, B., Matsui, T., Meyers, T., Oechel, W. C., Pielke, R. A., Wells, R., Wilson, K. & Xue, Y. K. (2004) Direct observations of the effects of aerosol loading on net ecosystem CO2 exchanges over different landscapes. *Geophysical Research Letters,* **31,** L20506.

Novick, K. A., Ficklin, D. L., Stoy, P. C., Williams, C. A., Bohrer, G., Oishi, A. C., Papuga, S. A., Blanken, P. D., Noormets, A., Sulman, B. N., Scott, R. L., Wang, L. & Phillips, R. P. (2016) The increasing importance of atmospheric demand for ecosystem water and carbon fluxes. *Nature Climate Change,* **6,** 1023-1027.

Pallardy, G. S. (2007) Chapter 12-Transpiration and Plant Water Balance. *Physiology of Woody Plants (Second Edition)***,** 269-308.

Pieruschka, R., Huber, G. & Berry, J. A. (2010) Control of transpiration by radiation. *Proceedings of the National Academy of Sciences of the United States of America,* **107,** 13372-13377.

Rabbel, I., Diekkruger, B., Voigt, H. & Neuwirth, B. (2016) Comparing Tmax Determination Approaches for Granier-Based Sapflow Estimations. *Sensors (Basel),* **16**.

Ramanathan, V., Crutzen, P. J., Kiehl, J. T. & Rosenfeld, D. (2001) Aerosols, climate, and the hydrological cycle. *Science,* **294,** 2119-24.

Rap, A., Scott, C. E., Reddington, C. L., Mercado, L., Ellis, R. J., Garraway, S., Evans, M. J., Beerling, D. J., MacKenzie, A. R., Hewitt, C. N. & Spracklen, D. V. (2018) Enhanced global primary production by biogenic aerosol via diffuse radiation fertilization. *Nature Geoscience,* **11,** 640-644.

Spinoni, J., Barbosa, P., Bucchignani, E., Cassano, J., Cavazos, T., Christensen, J. H., Christensen, O. B., Coppola, E., Evans, J., Geyer, B., Giorgi, F., Hadjinicolaou, P., Jacob, D., Katzfey, J., Koenigk, T., Laprise, R., Lennard, C. J., Kurnaz, M. L., Li, D. L., Llopart, M., McCormick, N., Naumann, G., Nikulin, G., Ozturk, T., Panitz, H. J., da Rocha, R. P., Rockel, B., Solman, S. A., Syktus, J., Tangang, F., Teichmann, C., Vautard, R., Vogt, J. V., Winger, K., Zittis, G. & Dosio, A. (2020) Future Global Meteorological Drought Hot Spots: A Study Based on CORDEX Data. *Journal of Climate,* **33,** 3635-3661.

Steiner, A. L. & Chameides, W. L. (2005) Aerosol-induced thermal effects increase modelled terrestrial photosynthesis and transpiration. *Tellus B: Chemical and Physical Meteorology,* **57,** 404-411.

Sulman, B. N., Roman, D. T., Yi, K., Wang, L., Phillips, R. P. & Novick, K. A. (2016) High atmospheric demand for water can limit forest carbon uptake and transpiration as severely as dry soil. *Geophysical Research Letters,* **43,** 9686-9695.

Urban, O., JanouŠ, D., Acosta, M., CzernÝ, R., MarkovÁ, I., NavrÁTil, M., Pavelka, M., PokornÝ, R., ŠPrtovÁ, M., Zhang, R. U. I., ŠPunda, V., Grace, J. & Marek, M. V. (2007) Ecophysiological controls over the net ecosystem exchange of mountain spruce stand. Comparison of the response in direct vs. diffuse solar radiation. *Global Change Biology,* **13,** 157-168.

Wang, F. L., Wang, H. & Wang, G. (2007) Photosynthetic responses of apricot (Prunus armeniaca

L.) to photosynthetic photon flux density, leaf temperature, and CO2 concentration. *Photosynthetica,* **45,** 59-64.

Wang, X., Wu, J., Chen, M., Xu, X., Wang, Z., Wang, B., Wang, C., Piao, S., Lin, W., Miao, G., Deng, M., Qiao, C., Wang, J., Xu, S. & Liu, L. (2018) Field evidences for the positive effects of aerosols on tree growth. *Glob Chang Biol,* **24,** 4983-4992.

Wang, Z., Wang, C., Wang, B., Wang, X., Li, J., Wu, J. & Liu, L. (2020) Interactive effects of air pollutants and atmospheric moisture stress on aspen growth and photosynthesis along an urban-rural gradient. *Environmental Pollution*.

Weston, D. J. & Bauerle, W. L. (2007) Inhibition and acclimation of C-3 photosynthesis to moderate heat: a perspective from thermally contrasting genotypes of Acer rabrum (red maple). *Tree Physiology,* **27,** 1083-1092.

Wu, J., Serbin, S. P., Xu, X., Albert, L. P., Chen, M., Meng, R., Saleska, S. R. & Rogers, A. (2017) The phenology of leaf quality and its within-canopy variation is essential for accurate modeling of photosynthesis in tropical evergreen forests. *Glob Chang Biol,* **23,** 4814-4827.

Xia, X., Li, Z., Wang, P., Chen, H. & Cribb, M. (2007) Estimation of aerosol effects on surface irradiance based on measurements and radiative transfer model simulations in northern China. *Journal of Geophysical Research,* **112,** D22S10.

Yoon, J., Burrows, J. P., Vountas, M., von Hoyningen-Huene, W., Chang, D. Y., Richter, A. & Hilboll, A. (2014) Changes in atmospheric aerosol loading retrieved from space-based measurements during the past decade. *Atmospheric Chemistry and Physics,* **14,** 6881-6902.

Yuan, W., Zheng, Y., Piao, S., Ciais, P., Lombardozzi, D., Wang, Y., Ryu, Y., Chen, G., Dong, W., Hu, Z., Jain, A. K., Jiang, C., Kato, E., Li, S., Lienert, S., Liu, S., Nabel, J. E. M. S., Qin, Z., Quine, T., Sitch, S., Smith, W. K., Wang, F., Wu, C., Xiao, Z. & Yang, S. (2019) Increased atmospheric vapor pressure deficit reduces global vegetation growth. *Science Advances,* **5,** eaax1396.

Zeppel, M., Tissue, D., Taylor, D., Macinnis-Ng, C. & Eamus, D. (2010) Rates of nocturnal transpiration in two evergreen temperate woodland species with differing water-use strategies. *Tree Physiology,* **30,** 988-1000.

Zhang, M., Yu, G.-R., Zhuang, J., Gentry, R., Fu, Y.-L., Sun, X.-M., Zhang, L.-M., Wen, X.-F., Wang, Q.-F., Han, S.-J., Yan, J.-H., Zhang, Y.-P., Wang, Y.-F. & Li, Y.-N. (2011) Effects of cloudiness change on net ecosystem exchange, light use efficiency, and water use efficiency in typical ecosystems of China. *Agricultural and Forest Meteorology,* **151,** 803-816.

Figures

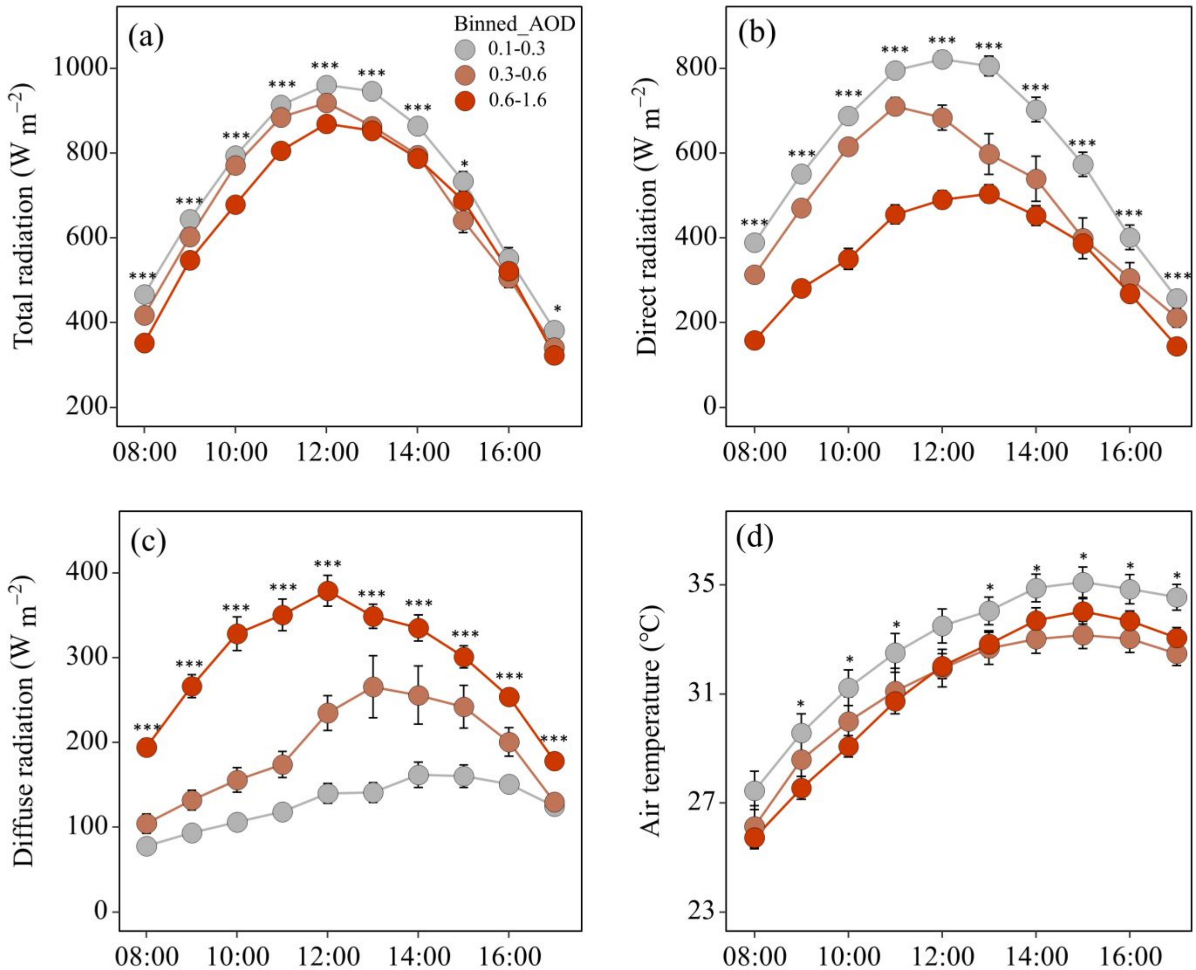

FIGURE 1 Diurnal course of (a) total radiation, (b) direct radiation, (c) diffuse radiation and (d) air temperature under natural variation in aerosol optical depth (AOD) values, binned into three intervals (0.1<AOD≤0.3, 0.3<AOD≤0.6, 0.6<AOD≤1.6). The data points represent the averaged observations for the given AOD bin under cloud-free skies. Error bars show the standard error of the mean. ANOVA test was used to assess the influences of AOD conditions on meteorological variables. Significance of differences between AOD bins for each hour is indicated by asterisks (*** $P < 0.001$; ** $P > 0.001$ & $P < 0.01$; * $P > 0.01$ & $P < 0.05$).

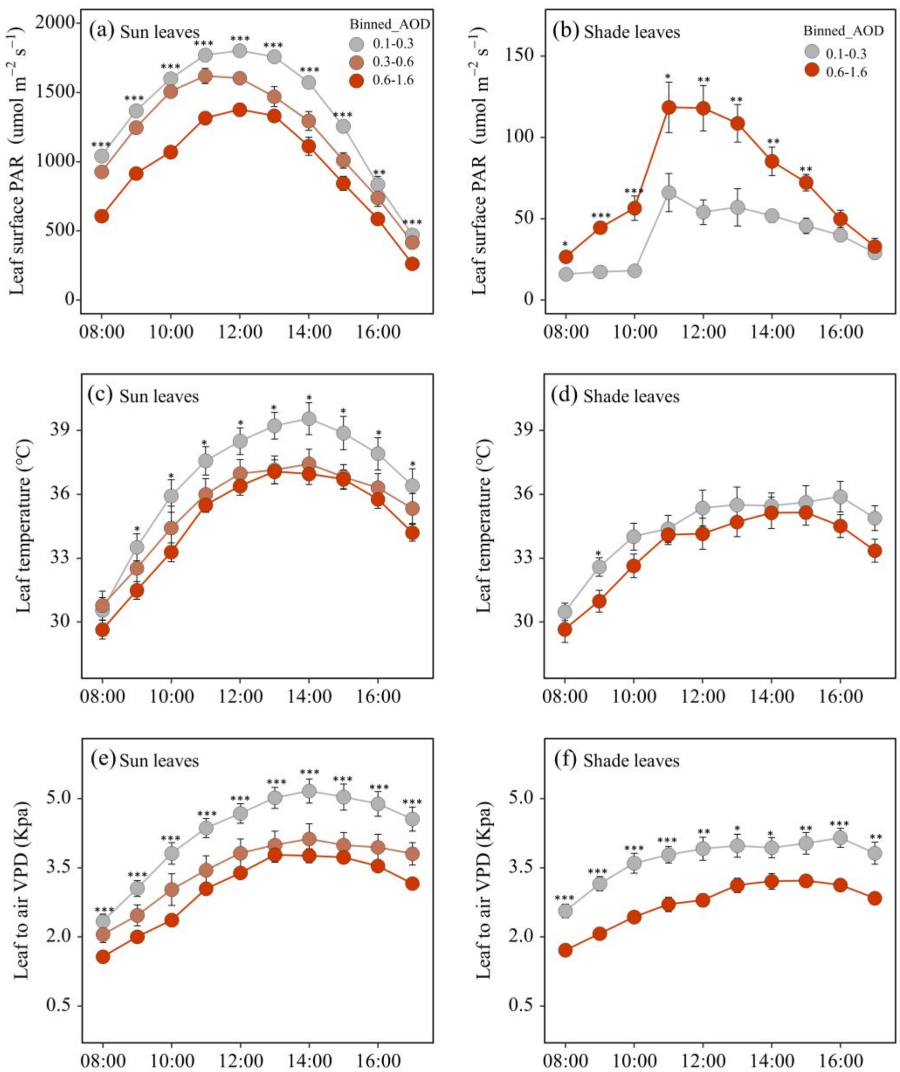

FIGURE 2 Diurnal course of photosynthetically active radiation (PAR), leaf-to-air vapor pressure deficit (VPD_{leaf}), and leaf temperature (T_{leaf}) for (a, c, e) sun leaves under natural variation in aerosol optical depth (AOD) values, binned into three intervals (0.1<AOD≤0.3, 0.3<AOD≤0.6, 0.6<AOD≤1.6), and for (b, d, f) shade leaves under different AOD values binned into two intervals (0.1<AOD≤0.3, 0.6<AOD≤1.6). The data points represent the averaged observations for the given AOD bin under cloud-free skies. Error bars show the standard error of the mean. ANOVA test was used to assess the influences of AOD conditions on leaf micrometeorological conditions. Significance of differences between AOD bins for each hour is indicated by asterisks (*** P < 0.001; ** P > 0.001 & P < 0.01; * P > 0.01 & P < 0.05).

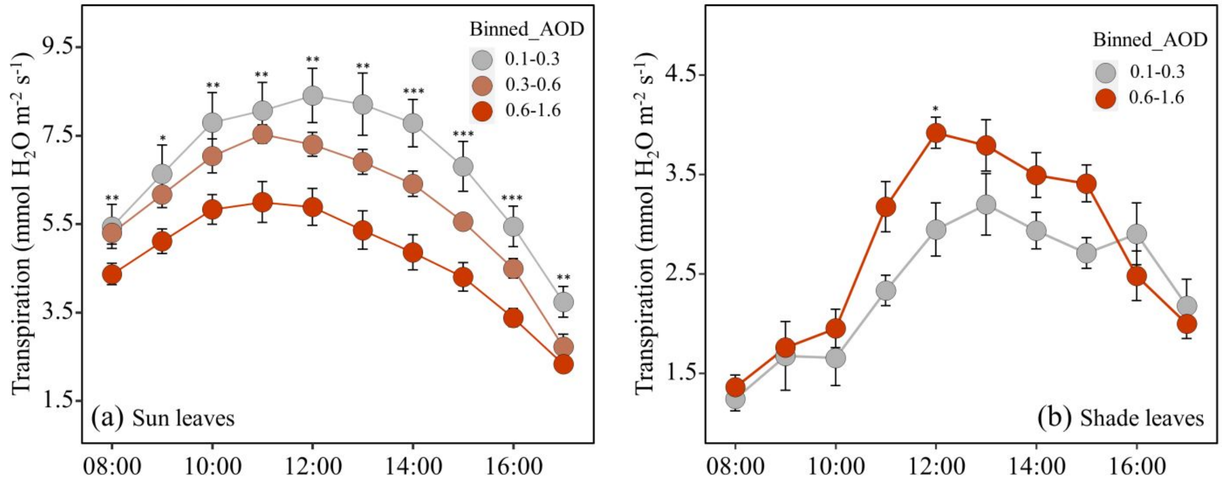

FIGURE 3 Diurnal course of transpiration rates of (a) sun leaves and (b) shade leaves under different aerosol-loading conditions. The data points represent the averaged observations for the given aerosol optical depth (AOD) bin under cloud-free skies. Error bars show the standard error of the mean. ANOVA test was used to assess the influences of AOD conditions on leaf transpiration. Significance of differences between AOD bins for each hour is indicated by asterisks (*** $P < 0.001$; ** $P > 0.001$ & $P < 0.01$; * $P > 0.01$ & $P < 0.05$).

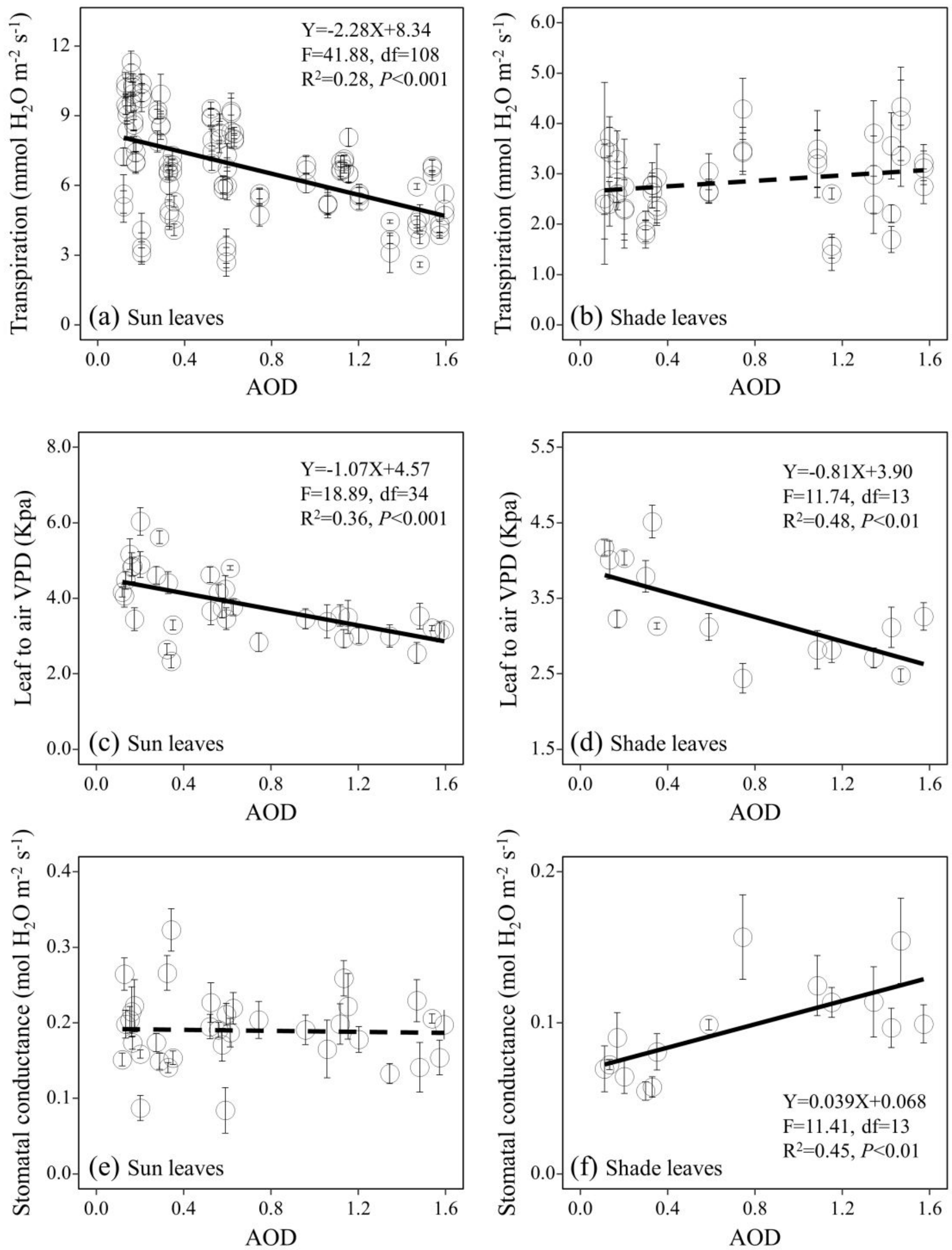

FIGURE 4 Response of leaf transpiration rate, leaf-to-air VPD and stomatal conductance of (a, c, e) sun and (d, e, f) shade leaves to AOD. Each circle represents the midday (solar zenith angle less than 40) average of the observations under cloud-free skies. Error bars show the standard error of the mean. Linear regression lines indicate significance (solid, $P < 0.05$; dashed $P > 0.05$). The results of the statistical test of linear regression are given in each panel.

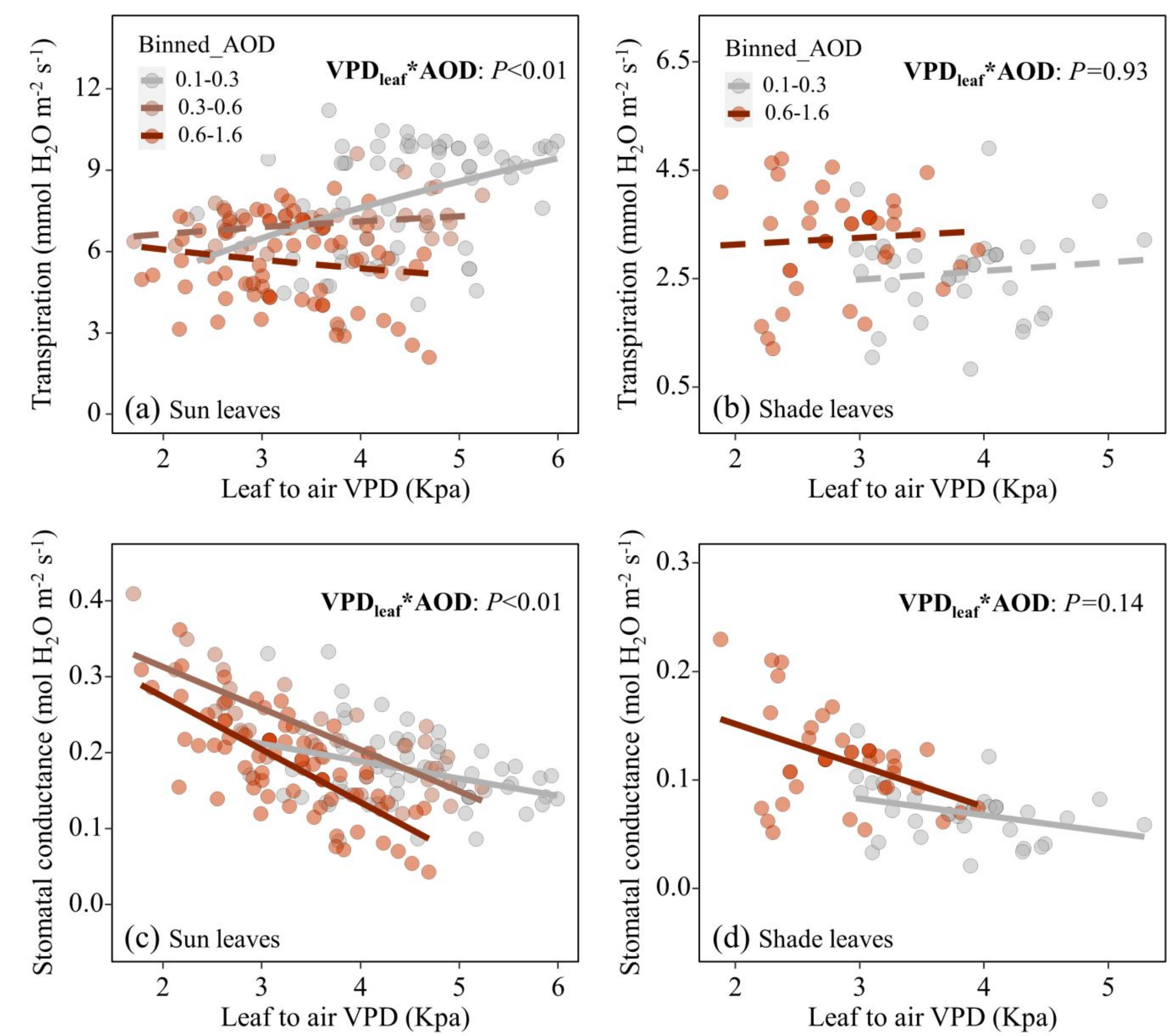

FIGURE 5 The response of leaf transpiration rate to VPD_{leaf} varies with aerosol loadings. Scatterplots of the relationship between (a, b) transpiration rate and VPD_{leaf} and (c, d) g_s and VPD_{leaf} at different aerosol bins for sun and shade leaves. Each point represents the hourly observation under a cloud-free sky with solar zenith angle <40. Linear regression lines indicate significance (solid, $P < 0.05$; dashed $P > 0.05$). Results for an ANCOVA of different slopes among aerosol optical depth (AOD) bins are displayed on each panel.

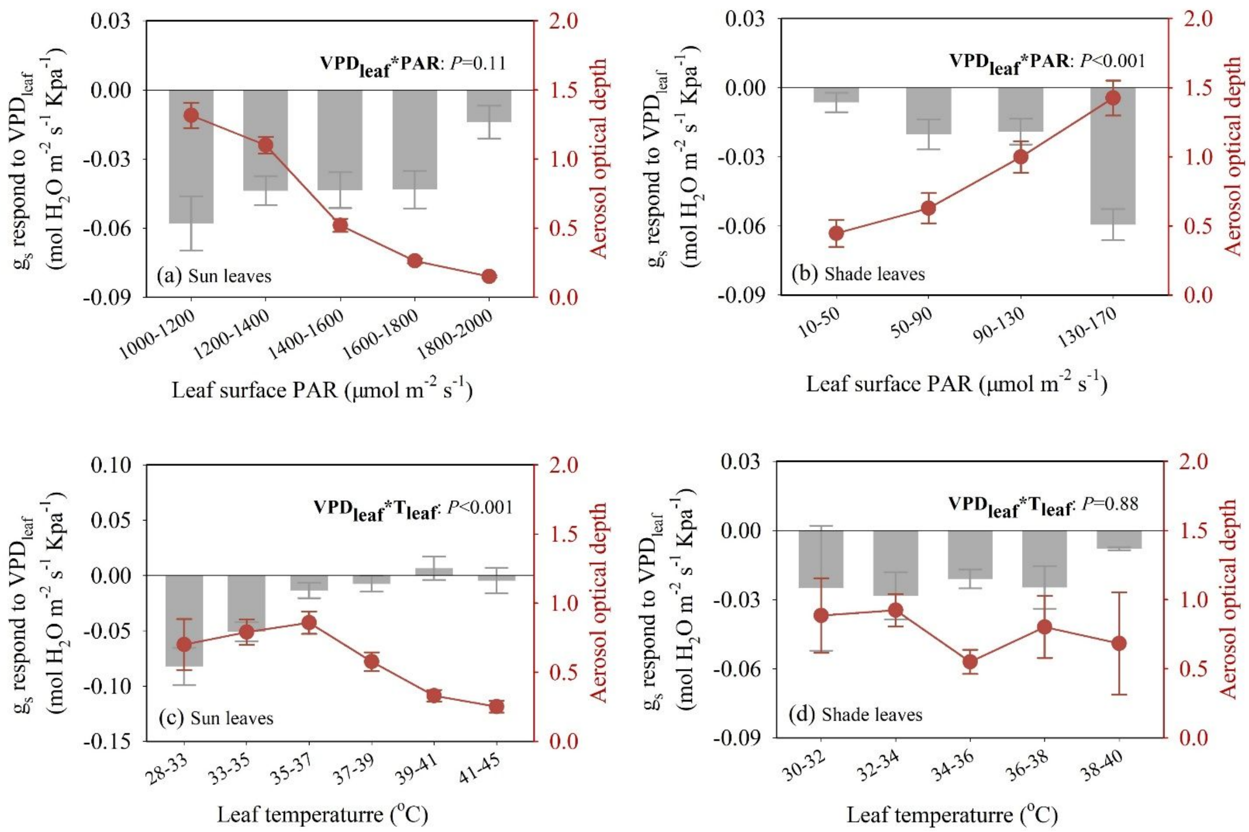

FIGURE 6 Sensitivity of g_s to VPD_{leaf} varies with PAR and T_{leaf}. The response of g_s to VPD_{leaf} of sun and shade leaves under different (a, b) PAR bins and (c, d) T_{leaf} bins. Bars represent the slopes of the linear regression of g_s against VPD_{leaf}, and error bars indicate the 95% confidence intervals for each slope. The dots indicate the mean of each aerosol optical depth (AOD) value of each bin. Results of ANCOVA for different slopes among PAR or T_{leaf} bins are shown in each panel.

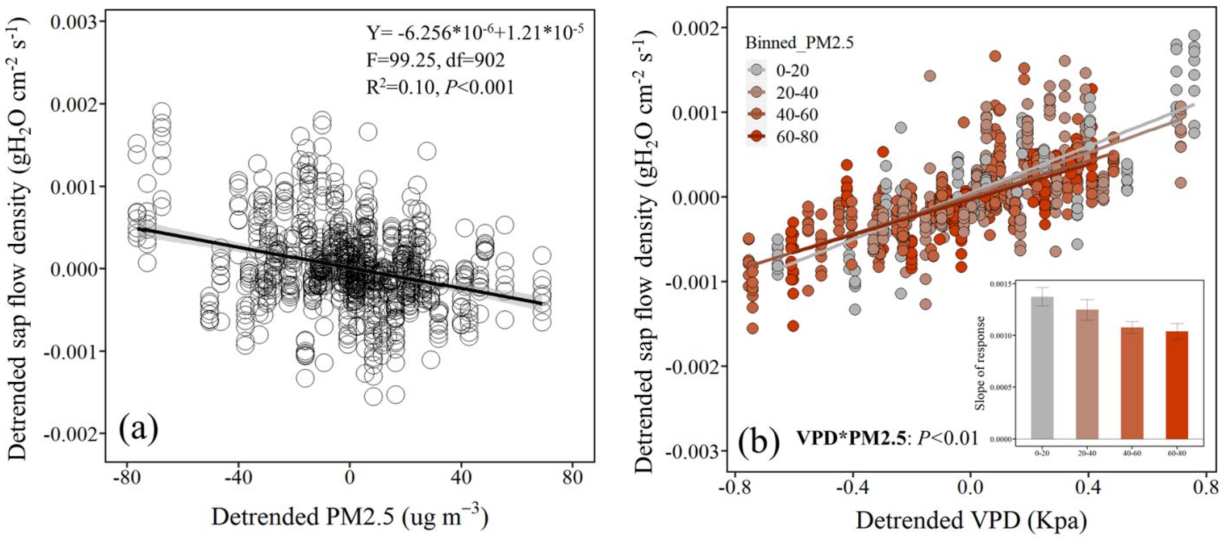

FIGURE 7 Aerosol effects on canopy transpiration and its response to air vapor pressure deficit. (a) Scatterplot of the relationship between sap flow density and PM2.5 concentration, the sap flow density, and PM2.5 concentration were both trend-decomposed using first-order difference. (b) Scatterplot of relationship between detrended sap flow density and detrended vapor pressure deficit under different PM2.5 bins. The data represented the first-order difference of daily average sap flow density, PM2.5 concentration, and vapor pressure deficit in cloud-free days. The inserted bar plot shows the slope of the regression between sap flow density and vapor pressure deficit, and the error bars were the standard error of the slope. ANCOVA results for different slopes among PM2.5 bins (VPD*PM2.5) are shown in the panel.

Supporting information

Title: Field evidence reveals conservative water use of poplars under high aerosol conditions in Beijing

Authors:

Bin Wang[1, 2], Zhenhua Wang[1, 2], Chengzhang Wang[1, 2], Xin Wang[1], Jing Li[1, 2], Zhou Jia[1, 2], Ping Li[1, 2], Jin Wu[3], Min Chen[4], Lingli Liu[1, 2*]

Author affiliations:

[1] State Key Laboratory of Vegetation and Environmental Change, Institute of Botany, Chinese Academy of Sciences, Xiangshan, Beijing 100093, China

[2] University of Chinese Academy of Sciences, Yuquanlu, Beijing 100049, China

[3] School of Biological Sciences, The University of Hong Kong, Pokfulam, Hong Kong, China

[4] Department of Forest and Wildlife Ecology, University of Wisconsin-Madison, Madison, Wisconsin, USA

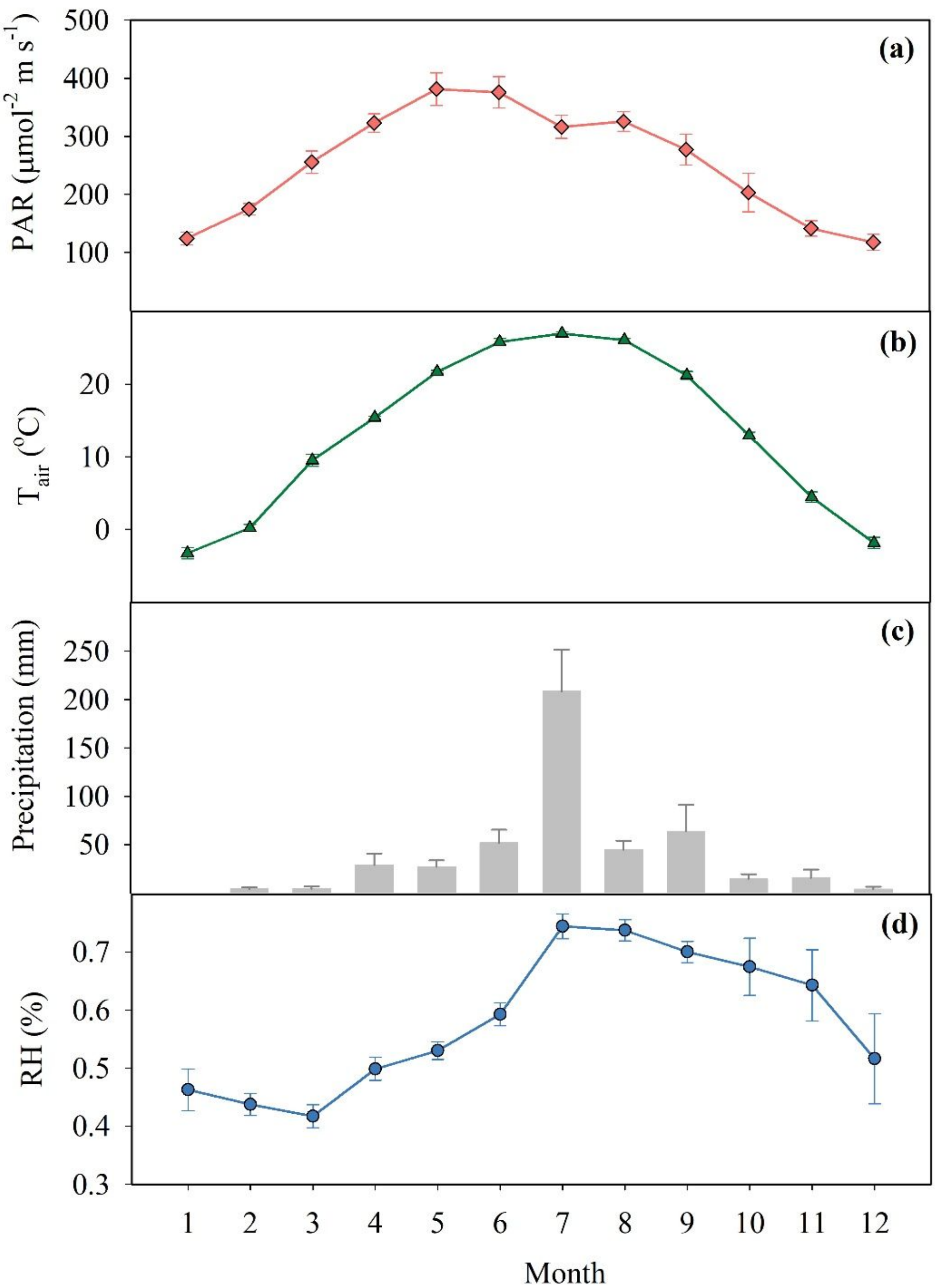

FIGURE S1 The mean monthly variations of (a) photosynthetically active radiation (PAR), (b) air temperature (T_{air}), (c) precipitation and (d) relative humidity (RH) during 2014 to 2018 in the study site. Error bars show the standard error of the mean.

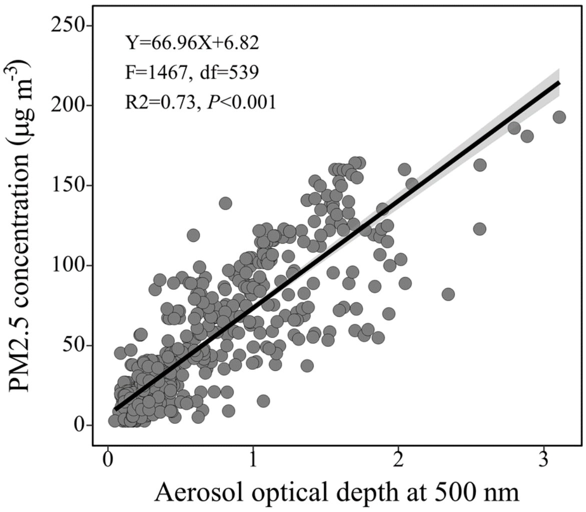

FIGURE S2 Relationship between PM2.5 concentration measured at the Beijing Municipal Environmental Monitoring Center and aerosol optical depth at 500 nm measured at the study site in July and August in 2014 and 2015. Each point represents an hourly observation under a clear sky. R^2, *P*-value, and equation of the linear regression are shown on the panel.

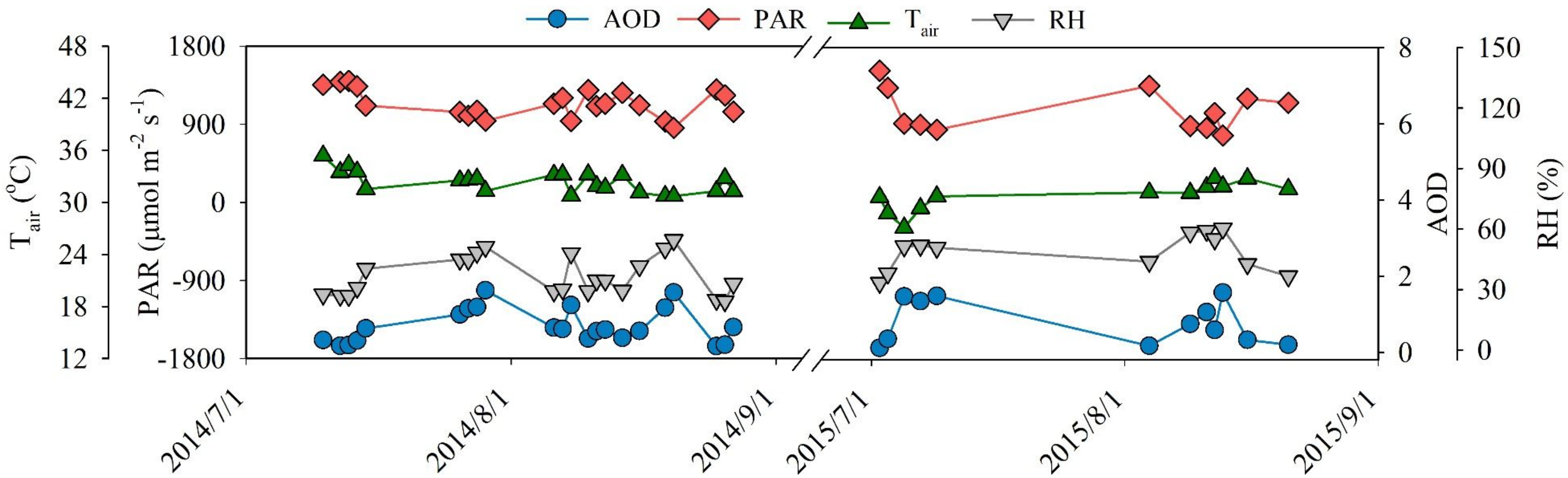

FIGURE S3 Dynamics of daily mean aerosol optical depth (AOD), photosynthetically active radiation (PAR), air temperature (T_{air}) and relative humidity (RH) during cloud-free days from July to August in 2014 and 2015.

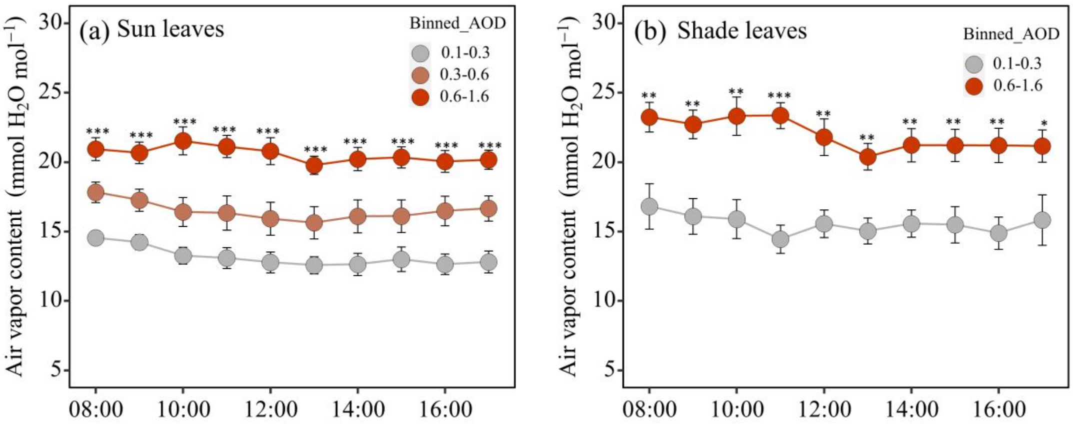

FIGURE S4 Diurnal dynamics of air water content (AVC) during measuring the transpiration of (a) sun and (b) shade leaves under different aerosol concentration conditions. The data points represent the averaged observations for the given aerosol optical depth (AOD) bin under cloud-free skies. Error bars show the standard error of the mean. ANOVA test was used to assess the influences of AOD levels on AVC. Significance of differences between AOD bins for each hour is indicated by asterisks (*** $P < 0.001$; ** $P > 0.001$ & $P < 0.01$; * $P > 0.01$ & $P < 0.05$).

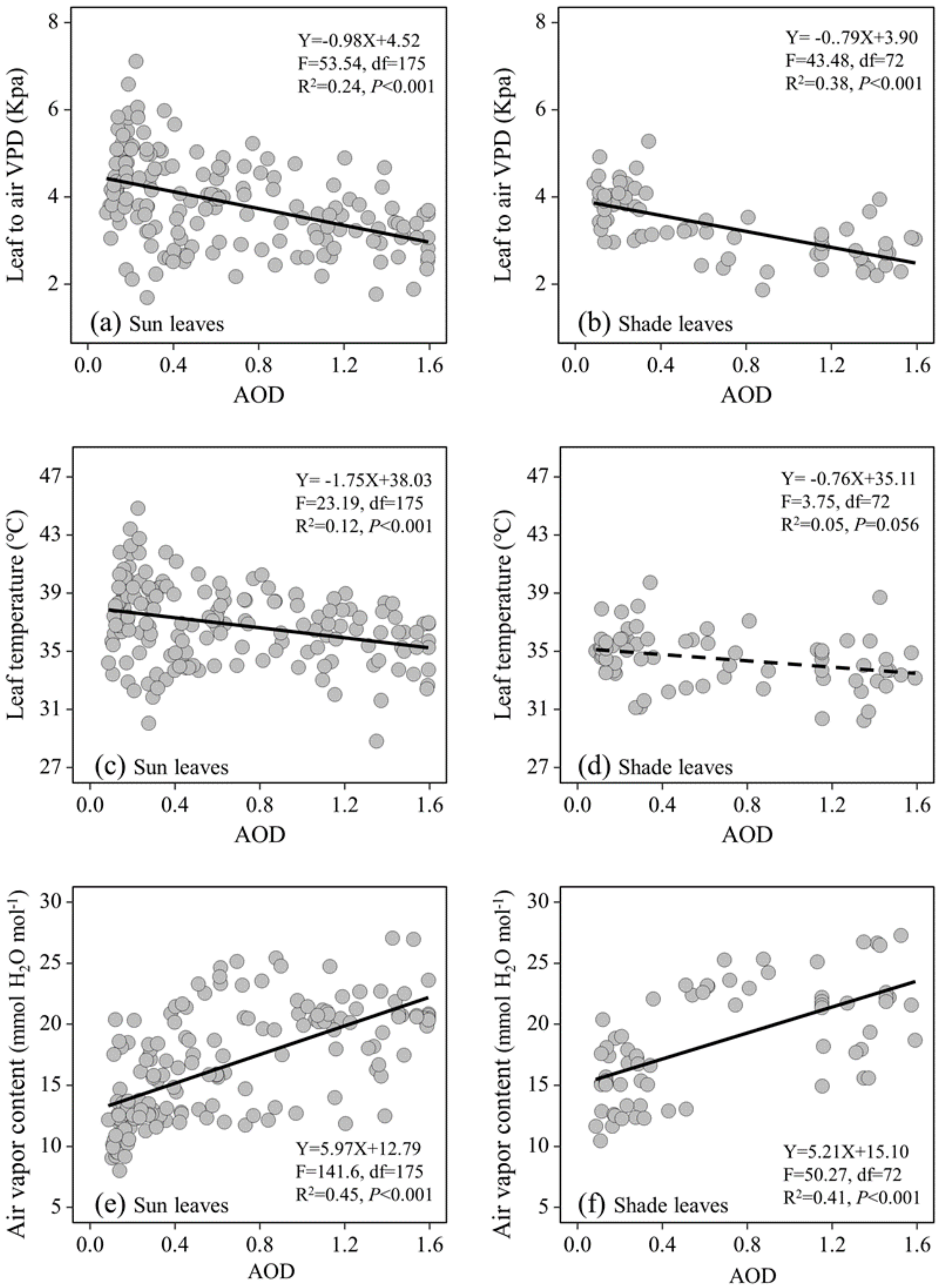

FIGURE S5 Aerosol effects on VPD_{leaf}. Response of VPD_{leaf}, T_{leaf} and AVC of (a, c, e) sun and (d, e, f) shade leaves to AOD. Points represent the observations around noon time (solar zenith angle less than 40, 11:00-14:00) under cloud-free skies. Linear regression lines indicate significance (solid, $P < 0.05$; dashed $P > 0.05$). The results of statistical test of linear regression are given in each panel.

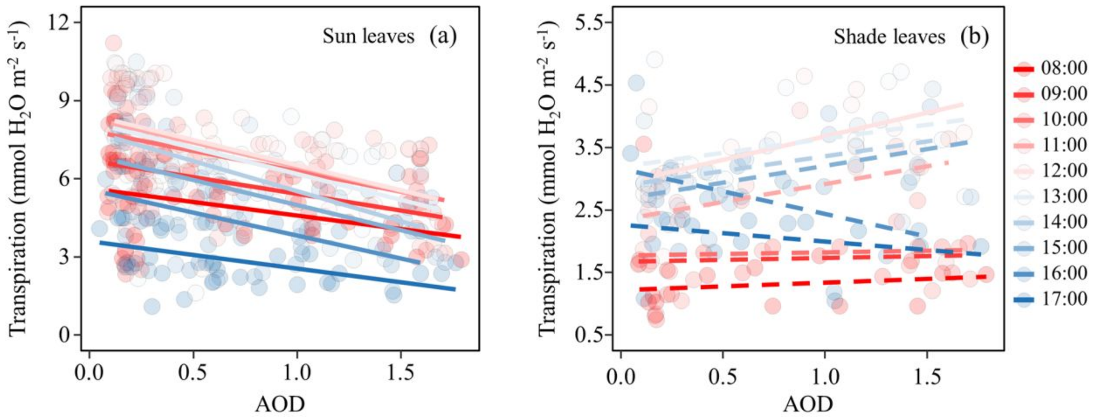

FIGURE S6 Changes of leaf transpiration under natural variation in aerosol optical depth (AOD) in a diurnal course for (a) sun and (b) shade leaves. The data points represent the observations under cloud-free skies. Linear correlation was used to assess the relationships between AOD and leaf transpiration. The solid lines indicate significance at $P < 0.05$ level, and the dashed lines indicate non-significant relationships ($P > 0.05$). The colors from red to blue indicate the hours from 08:00 to 17:00.

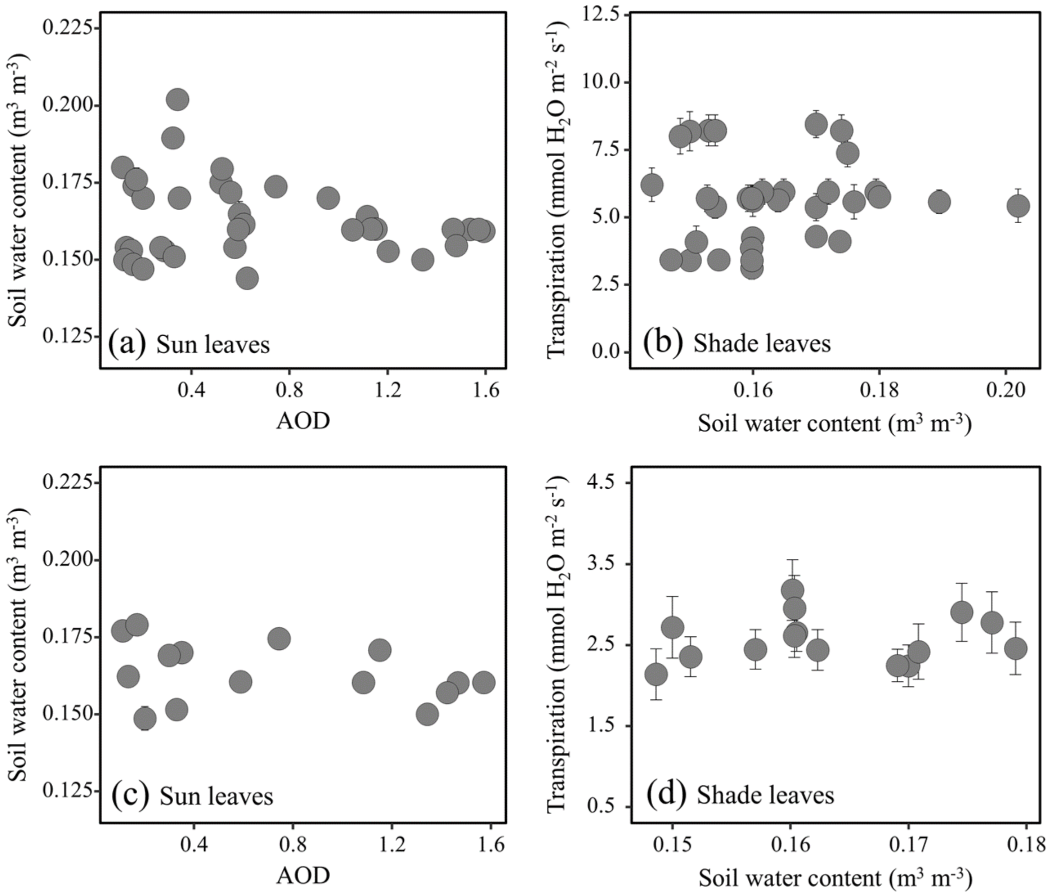

FIGURE S7 Effects of soil water content on leaf transpiration rate under different aerosol concentrations. Relationship between soil water content and AOD during observations for (a) sun and (c) shade leaves. Relationship between transpiration rate and soil water content for sun (b) and (d) shade leaves. Each point represents daily averaged observations during the measurement of leaf transpiration rate. Error bars show the standard error of the mean.

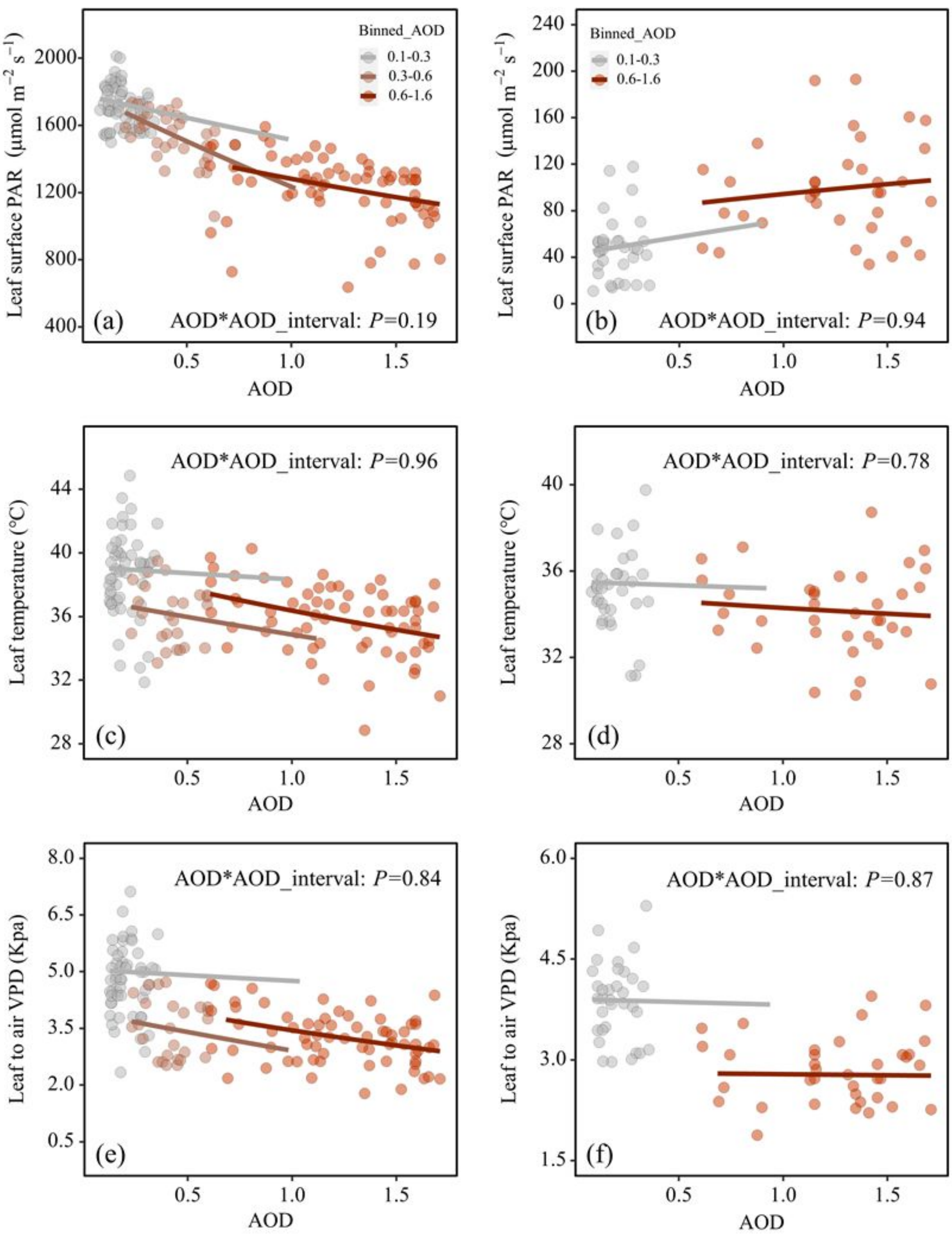

FIGURE S8 Aerosol effects on leaf surface PAR, T_{leaf} and $VPD_{leaf.}$ Analysis of covariance (ANCOVA) was used to compare the slopes of AOD vs microclimate (PAR, T_{leaf} and VPD_{leaf}) under three AOD intervals. The *P* values of AOD*AOD interval indicate that the microclimate variables show similar response to changes in AOD under three different AOD conditions.

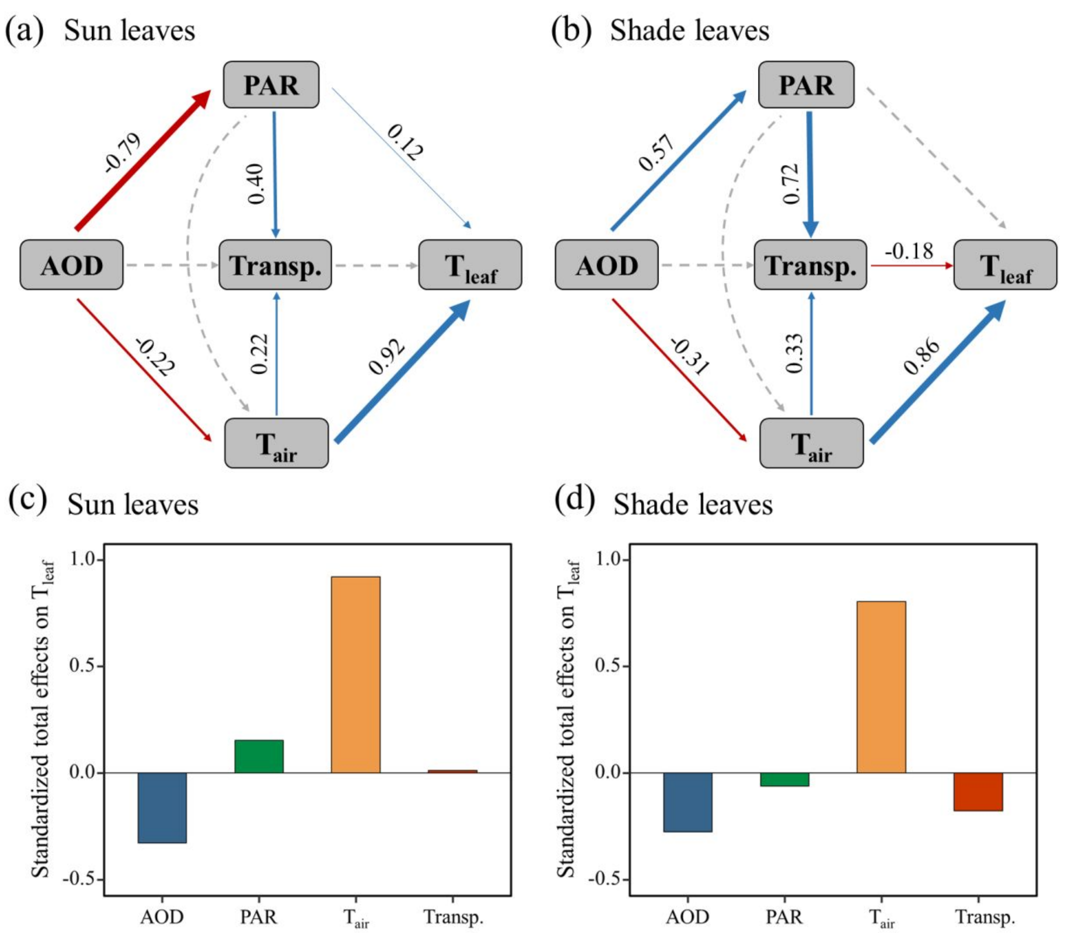

FIGURE S9 Structural equation models of aerosol effect on leaf temperature of (a) sun and (b) shade leaves. Standardized total effects of aerosol optical depth (AOD), meteorological factors and leaf transpiration on (c) sun and (d) shade leaf temperature. Blue and red lines indicate significantly positive and negative relationships between two factors. The effect size of the relationship indicated by standardized path coefficients (numbers adjacent to line) and represented by the width of lines. The model goodness of fits was suggested by X^2 and P-values (a: X^2=1.13, P=0.29; b: X^2=0.74, P=0.39). Variable abbreviations: AOD: aerosol optical depth; PAR: leaf received photosynthetically active radiation; T_{air}: air temperature; Transp.: leaf transpiration rate; T_{leaf}: leaf temperature.

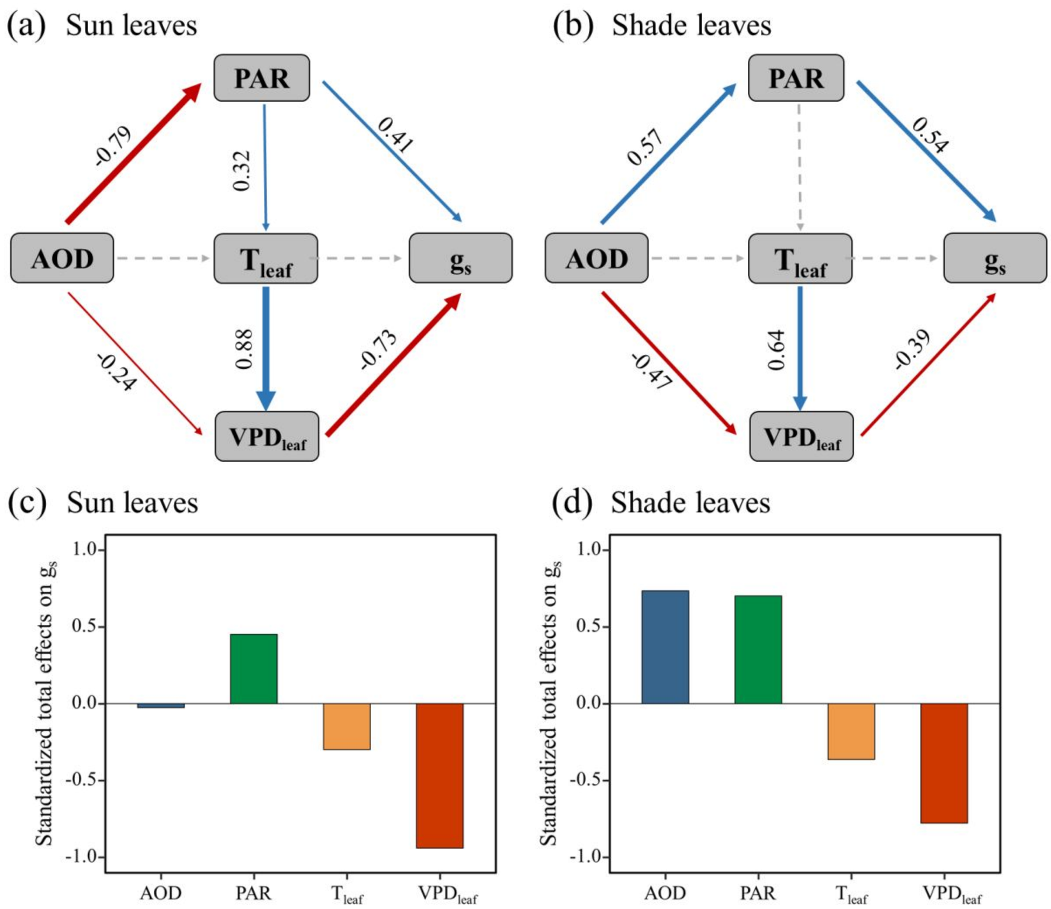

FIGURE S10 Structural equation model of aerosol effect on g_s of (a) sun and (b) shade leaves. Standardized total effects of aerosol optical depth (AOD) and meteorological factors on (c) sun and (d) shade leaf g_s. Blue and red lines indicate significantly positive and negative relationships between two factors. Dash lines indicate non-significant relationships (P>0.05). The effect size of the relationship indicated by standardized path coefficients (numbers adjacent to line) and represented by the width of lines. The model goodness of fits was suggested by X^2 and P-values (a: X^2=1.44, P=0.49; b: X^2=9.30, P=0.06). Variable abbreviations: AOD: aerosol optical depth; PAR: leaf received photosynthetically active radiation; T_{leaf}: leaf temperature; VPD_{leaf}: leaf to air vapor pressure deficit; g_s: stomatal conductance for water.

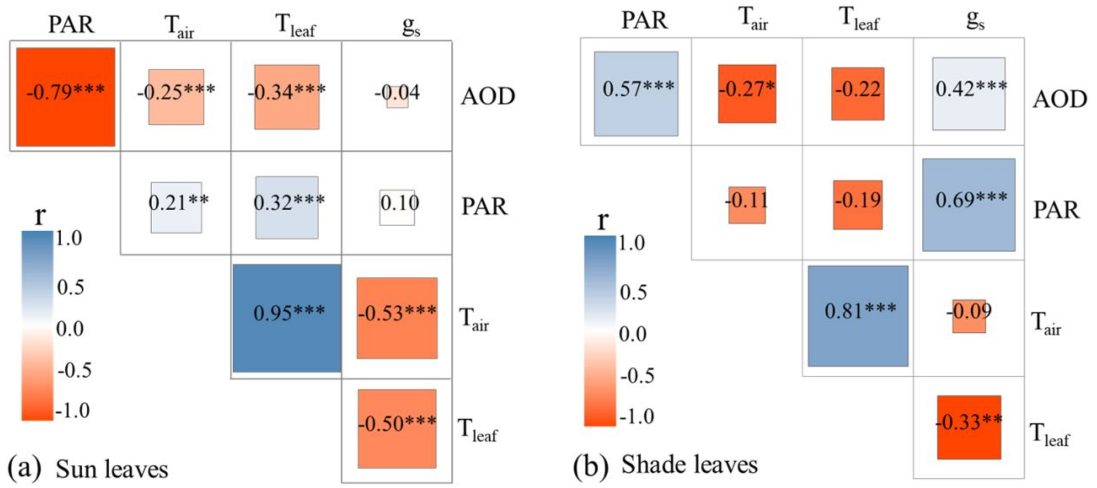

FIGURE S11 Correlations among aerosol optical depth (AOD), photosynthetically active radiation (PAR), air temperature (T_{air}), leaf temperature (T_{leaf}) and stomatal conductance (g_s) during the midday for (a) sun and (b) shade leaves. The numbers indicate the correlation coefficient for a given pair of variables. The statistical significance of the correlation is indicated by asterisks (*** $P < 0.001$; ** $P > 0.001$ & $P < 0.01$; * $P > 0.01$ & $P < 0.05$).

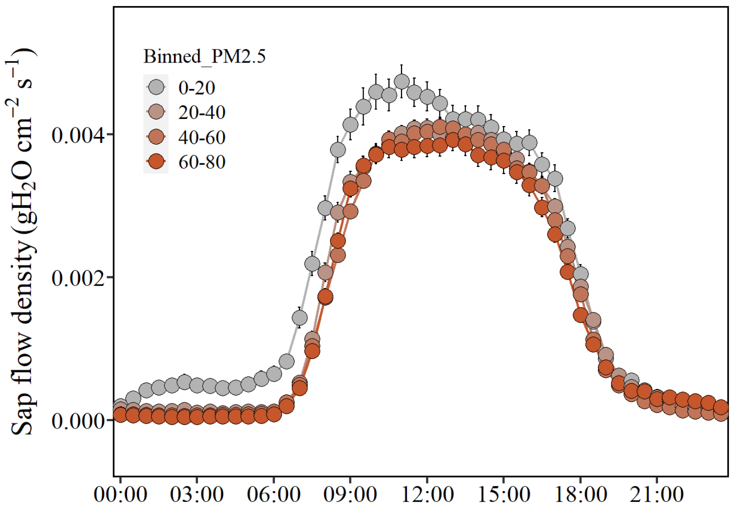

FIGURE S12 Diurnal dynamics of sap flow density under different aerosol concentration conditions. The data points represent averaged observations for given PM2.5 bins under cloud-free skies. Error bars show the standard error of the mean.

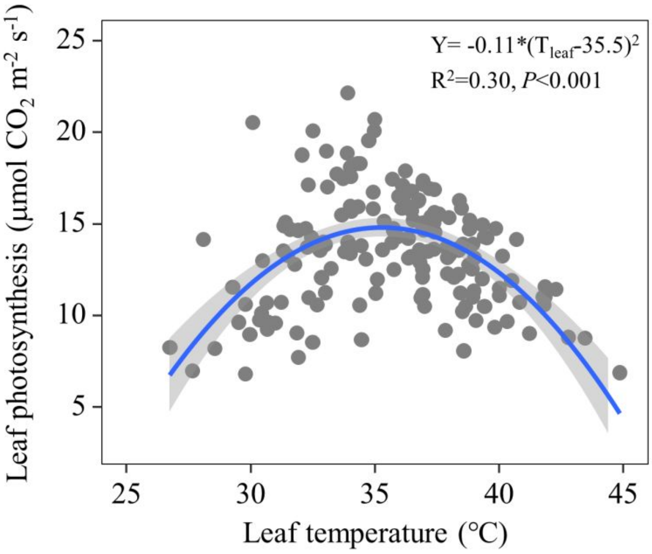

FIGURE S13 The relationship between leaf temperature and photosynthesis of sun leaves.

TABLE S1 The climate conditions and characteristics of poplar trees during the measurements of leaf transpiration and sap flow density. Precipitation indicates the accumulated precipitation, air temperature (T_{air}), total radiation, relative humidity (RH), diameter at the breast height (DBH), sapwood thickness at DBH, tree height and leaf area index (LAI) are the means during the measurements (July-August). Numbers in parentheses indicate standard error of the mean.

Year	Measurements	Precipitation (mm)	T_{air} (℃)	Radiation (W m^{-2})	RH (%)	DBH (mm)	Sapwood thickness (mm)	Height (m)	LAI (m^2 m^{-2})	Number of cloud-free days
2014	Sun leaf transpiration	186.2	26.63(0.42)	232.14(5.49)	72.97(2.15)	87.25 (3.67)	35.56 (2.29)	7.75 (0.24)	4.46 (0.12)	24
2015	Sun and shade leaf transpiration	260.5	25.64(0.27)	242.81(5.68)	67.99(1.42)	92.53 (4.34)	37.67 (2.56)	8.20 (0.27)	4.88 (0.16)	15
2017	Sap flow density	392.6	26.07(0.35)	202.40(5.08)	72.81(1.27)	84.44 (3.46)	34.44 (2.21)	7.26 (0.26)	4.08 (0.09)	17
2018	Sap flow density	379.8	27.07(0.28)	203.20(4.54)	78.11(1.33)	89.28 (4.12)	36.37 (2.47)	7.98 (0.22)	4.54 (0.10)	23